

Part I
Fundamental Aspects of Microwave Irradiation
in Organic Chemistry

1

Microwave–Materials Interactions and Dielectric Properties: from Molecules and Macromolecules to Solids and Colloidal Suspensions

Didier Stuerge

1.1 Fundamentals of Microwave–Matter Interactions

The objective of the first part of the book is to explain in a chemically intelligible fashion the physical origin of microwave–matter interactions and in this chapter especially the theory of dielectric relaxation of polar molecules. This third revised edition contains approximately 30% of new material in order to cover a large area of reaction media able to be heated by microwave irradiation. Colloidal suspensions and highly functional polymers are now included. The accounts presented in the various chapters are intended to be illustrative rather than exhaustive. They are planned to serve as introductions to the various aspect of interest for comprehensive microwave heating. In this sense, the treatment is selective and to some extent arbitrary. Hence the reference lists contain historical papers and valuable reviews to which the reader anxious to pursue further particular aspects should certainly turn.

It is the author's conviction, confirmed over many years of teaching experience, that it is much safer – at least for those who rate not trained physicists – to deal intelligently with oversimplified models than to use sophisticated methods which require experience before becoming productive. However, and in response to comments on the first and second editions, the author has given more technical comments in relation to a better understanding of concepts and ideas. These paragraphs can be omitted depending on the level of experience of the reader. They are preceded by two type of logo: ✂ TOOLS and ⚙ CONCEPTS.

After some considerations relating to the history and the position in the spectrum of microwaves, notions of polarization and dielectric loss will be examined. The orienting effects of the electric field and the physical origin of dielectric loss will be analyzed, in addition to transfers between rotational states and vibrational states within condensed phases.

Dielectric relaxation and dielectric losses of pure liquids, ionic solutions, solids, polymers, and colloids will be discussed. The effect of electrolytes, relaxation of

defects within crystals lattices, adsorbed phases, interfacial relaxation, space-charge polarization, and the Maxwell–Wagner effect will be analyzed.

In this third revised edition, key ingredients for mastery of chemical microwave processes are given in a specific chapter (see Chapter 3). The thermal conversion parameters, thermodynamic aspects, and athermal effects will be described.

1.1.1

Introduction

According to the famous chemistry dictionary of P. Macquer published in 1766, “*All chemistry operations could be reduced to decomposition and combination; hence fire appears as a universal agent in chemistry as in Nature*” [1]. So far, heating still remains the primary means of stimulating chemical reactions which proceed slowly under ambient conditions; several other stimulating techniques such as photochemical, ultrasonic, high-pressure, and plasma methods could also be used. In this book, we describe results obtained with the help of microwave heating. Microwave heating or dielectric heating is an alternative to conventional conductive heating. This heating technique uses the ability of some products (liquids and solids) to transform electromagnetic energy into heat. This *in situ* mode of energy conversion is very attractive for chemistry applications and material processing.

Whereas the effect of the temperature on reaction rate is well known, and is very easy to express, the problem is very different for the effects of electromagnetic waves. What can be expected from the orienting action of electromagnetic fields at molecular levels? Are electromagnetic fields able to enhance or to modify collisions between reagents? All these questions are raised when microwave energy is used in chemistry.

1.1.1.1 History

How It All Began There is some controversy about the origins of the microwave power cavity called the *magnetron*: the high-power generator of microwave power. The British were particularly forward-looking in deploying radar for early warning air defense with a system called *Chain Home*, which began operation in 1937. Originally operating at 22 MHz, frequencies were subsequently increased to 55 MHz. The superiority of still higher frequencies for radar was appreciated theoretically but a lack of suitable detectors and of high-power sources prevented the development of microwaves. Magnetrons provide staggering amounts of output power (e.g., 100 kW on a pulse basis) for radar transmitters. The earliest description of magnetron, a diode with a cylindrical anode, was published by A.W. Hull in 1921 [2, 3]. From a practical point of view, it was developed by Randall and Booth at the University of Birmingham in England around 1940 [4]. On 21 February 1940, they verified their first microwave transmissions: 500 W at 3 GHz. A prototype was brought to the USA in September of that year in order to define an agreement whereby US industrial capability would undertake the development of microwave radar. In November 1940, the Radiation Laboratory was established at

the Massachusetts Institute of Technology to exploit the microwave radar. More than 40 types of tubes were produced, particularly in the S-band (i.e., 300 MHz). The growth of microwave radar is linked with Raytheon Company and P.L. Spencer, who found the key for mass production. Microwave techniques were developed during and just prior to World War II when most of the efforts were concentrated on the design and manufacture of microwave navigation and communications equipment for military use. Originally, microwaves played a leading role during the World War II, especially in the Battle of Britain where English planes could fight one against three thanks to radar. It hardly seems surprising that with all this magnetron manufacturing expertise microwave cooking would be invented at Raytheon and that the first microwave oven would be built there.

From the beginning, the heating capability of microwave power was recognized by scientists and engineers, but radar development had top priority. A new step began with the publication of microwave heating patents by Raytheon on 9 October 1945. Others patents followed as problems were encountered and solutions found. Probably the first announcement of a microwave oven was a magazine article concerning a newly developed “Radarange” for airline use [5, 6]. This device, it was claimed, could bake biscuits in 29 s, cook hamburgers in 35 s, and grill frankfurter in 10 s. This name Radarange almost became the generic name for microwave ovens. A picture of an early prototype is shown in a book by Decareau and Peterson [7]. This first commercial microwave oven was developed by P.L. Spencer of Raytheon in 1950 [8]. Legend has it that P.L. Spencer, who studied high-power microwave sources for radar applications, observed melting of a chocolate bar put in his pocket when next to a source of microwave power. Another story says that M.P.L. Spencer had some popcorn in his pocket that began to pop as he was standing alongside a live microwave source [7].

These first oven prototypes were placed in laboratories and kitchens throughout the USA to develop microwave cooking technology. The transition between the crude aircraft heater to a domestic oven took almost 8 years. The turning point of the story of the microwave oven was in 1965. This year was the beginning of a flurry of manufacturing activity and the issue of hundreds of patents on various aspects of oven design, processes, packaging, food products, appliances, and techniques. The widespread domestic use of microwave ovens occurred during the 1970s and 1980s as a result of the generation of the mass market and also of Japanese technology transfer and global marketing.

From Cooking to Microwave Processing The first studies of the effect of microwave heating were carried out at the Massachusetts Institute of Technology’s Department of Food Technology on bleaching of vegetables, coffee roasting, and the effect of cooking and baking upon vitamin retention [9]. A comparison between microwave and conventional freeze-drying of foods was made by Jackson *et al.* [10]. The Food Research Laboratory of Raytheon carried out extensive studies that led to the first microwave freeze-drying pilot plant unit [11–16].

Microwave processing began on a commercial scale in the early 1960s when Cryodry Corporation of San Ramon, CA, introduced the first conveyORIZED system

for sale. The first market was the potato chip finish drying process with several systems operating in the USA and Europe [17, 18]. These systems operated at 915 MHz. A number of 5–10 kW pilot plant conveyor systems were sold during this time to food manufacturers by Raytheon and Litton Industries Atherton Division. These systems all operated at 2450 MHz. One poultry processing system [19] had a total of 130 kW, split between two conveyor units. This system combined microwave power and saturated steam to precook poultry parts for the institutional and restaurant food service markets. This system operated at 2450 MHz.

Among food applications, microwave tempering of frozen foods, pasta drying, precooking of bacon, poultry processing, meat pattie cooking, frankfurter manufacturing, drying egg yolk paste, baking, sterilization, potato processing, cocoa bean roasting, and vacuum drying can be cited [7, 20]. Curiously, industrial applications of microwave heating were initiated by the domestic oven.

Early Foundations Many histories of electromagnetic waves and especially microwaves begin with the publication of the *Treatise on Electricity and Magnetism* by James Clerk Maxwell in 1873. These equations were initially expressed by Maxwell in terms of quaternions. O. Heaviside and J.W. Gibbs later rejected quaternions in favor of classical vector formulation to frame Maxwell's equations in their well-known form. Students and users of microwave heating, perhaps bemused by terms such as divergence, gradient, and curl, often fail to appreciate just how revolutionary this insight was. The existence of electromagnetic waves that travel at the speed of light were predicted by arbitrarily adding an extra term (the displacement current) to the equations that described all previously known electromagnetic behavior. According to T.H. Lee [21], and contrary to the standard story presented in many textbooks, Maxwell did not introduce the displacement current to resolve any outstanding conundrums but was apparently inspired more by an esthetic sense that Nature simply should provide for the existence of electromagnetic waves. Maxwell's work was magical and arguably ranks as the most important intellectual achievement of the nineteenth century. According to the Nobel Prize physicist R. Feynman, future historians would still marvel at this work, long after another event of that time, the American Civil War, had faded into merely parochial significance [21].

Maxwell died in 1879 (aged 48 years), and H. Von Helmholtz sponsored a prize for the first experimental evidence of Maxwell's predictions. H. Hertz verified that Maxwell's predictions were correct in 1888 at the Technische Hochschule in Karlsruhe. According to T.H. Lee [21] another contestant in the race was O. Lodge, a professor at University College in Liverpool, having published his own experimental evidence one month before Hertz. *Hertz* is the German word for *heart* and the human heart beats about once per second, so it is perhaps all for the best that Lodge did not win the race and "lodgeian waves" with frequencies measured in "gigalodges" will never see the light of day.

How was it possible to produce and detect electromagnetic waves in the 1880s? The first experiment of Hertz produced microwaves (frequency close to gigahertz). His basic transmitter–receiver is shown in Figure 1.1. The generator is a Ruhmkorff

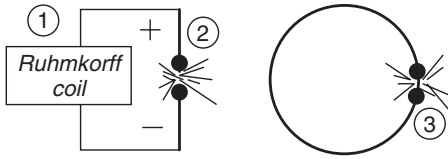


Figure 1.1 Spark transmitter and receiver of Hertz's original experiment.

coil or a transformer able to produce very high tension (1). This device is very close to the starter of a car.

The high voltage in the secondary causes a spark discharge within straight wire connections in order to produce the desired resonant frequency (2). The detector is a ring antenna with a spark gap (3). Detection is based on induction of sufficient voltage in the ring antenna to produce visible spark. Hertz demonstrated the essential physics of wave phenomena such as polarization and reflection. He died of blood poisoning from an infected tooth in 1894 at the age of 36 years. Commercial applications of wireless were developed by G. Marconi. Many details of the whole history of microwave technology can be found in [21].

1.1.1.2 The Electromagnetic Spectrum

In the electromagnetic spectrum, microwave radiation takes place in a transition area between infrared radiation and radiofrequency as illustrated in Figure 1.2. The wavelengths are between 1 cm and 1 m and frequencies between 300 GHz and 300 MHz.

The term *microwave* denotes techniques and concepts used in addition to a range of frequencies. Microwaves may be transmitted through hollow metallic tubes and

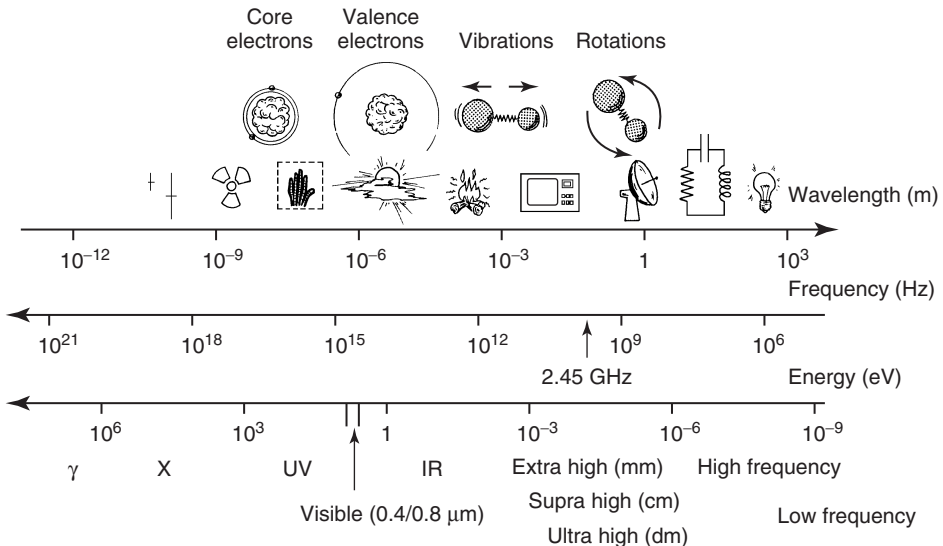


Figure 1.2 The electromagnetic spectrum.

may be focused into beams by the use of high-gain antennas. Microwaves also change direction on traveling from one dielectric material into another similarly to the way in which light rays are bent (refracted) when they pass from air into water. Microwaves travel in the same manner as light waves; they are reflected by metallic objects, absorbed by some dielectric materials, and transmitted without significant absorption through other dielectric materials. Water, carbon, and foods with high water contents are good microwave absorbers, whereas ceramics and most thermoplastic materials lead to slight microwave absorption.

The fundamental connection between energy E , frequency ν , wavelength λ , and circular frequency ω is given by

$$E = \hbar\omega = h\nu = \frac{hc}{\lambda} \quad (1.1)$$

In order to avoid interference with telecommunications and cellular phone frequencies, heating applications need to use ISM bands (industrial scientific and medical frequencies), which are 27.12 MHz, 915 MHz, and 2.45 GHz (i.e., 11.05 m, 37.24 m, and 12.24 cm for wavelengths, respectively). Domestic ovens and laboratory systems generally work at 2.45 GHz. At frequencies below 100 MHz, where conventional open-wire circuits are used, the technique will be referred to as *radiofrequency heating*. The object to be heated is placed between the two electrodes of a capacitor. However, at frequencies above 500 MHz, wired circuits cannot be used and the power is transferred to the applicator containing the material to be processed. Hence the microwave applicator is a metallic box in which the object to be heated is placed. These operating conditions will be referred to as *microwave heating processes*. In the microwave band, the wavelength is of order of the size of production and transmission elements. Therefore, elements cannot be considered as points in comparison with wavelength as is done in circuit theory. In the same way, it is impossible to consider them as far bigger than the wavelength as is done in geometric optics. Hence, because of the position of microwaves in the electromagnetic spectrum, both quantum mechanics (corpuscular aspect) and Maxwell equations (wave-like aspect) will be used. Detailed analysis of these phenomena is beyond the scope of this chapter.

1.1.1.3 What About Chemistry: Energetic Comments

It is well known that γ or X photons have energies suitable for excitation of inner or core electrons. We can use ultraviolet and visible radiation to initiate chemical reactions (photochemistry, valence electrons). Infrared radiation only excites bond vibrations, whereas microwaves excite molecular rotations.

Table 1.1 gives a comparison between energies associated with chemical bonds and Brownian motion. The microwave photons corresponding to the frequency used in microwave heating systems such as domestic and industrial ovens have energies close to 0.00001 eV (2.45 GHz, 12.22 cm). According to these values, the microwave photon is not sufficiently energetic to break hydrogen bonds. Furthermore, its energy is much smaller than that of Brownian motion, and it obviously cannot induce chemical reactions. If no bond breaking can occur by direct

Table 1.1 Brownian motion and bond energies.

	Brownian motion	Hydrogen bonds	Covalent bonds	Ionic bonds
Energy (eV)	≈0.017 (200 K)	~0.04–0.44	~4.51 (C–H) ~3.82 (C–C)	~7.6
Energy (kJ mol ⁻¹)	1.64	~3.8–42	~435 (C–H) ~368 (C–C)	~730

absorption of electromagnetic energy, then what can be expected from orienting effects of electromagnetic fields at molecular levels? Are electromagnetic fields able to enhance or to modify collisions between reagents? Do reactions proceed with the same reaction rate with and without electromagnetic irradiation for the same bulk temperature? In the following, the orienting effects of the electric field and the physical origin of the dielectric loss, and also transfers between rotational and vibrational states in condensed phases and thermodynamic effects of electric fields upon chemical equilibrium, will be analyzed.

✂ TOOLS More About Energy Partition of Molecular Systems

Rotational motions of molecular systems are much slower than vibrational motions of the relatively heavy nuclei forming chemical bonds, and even slower than electronic motions around nuclei. These vastly differing time scales of the various types of motions lead to a natural partitioning of the discrete energy spectrum of matter into progressively smaller subsets associated with electronic, vibrational, and rotational degrees of freedom.

The Born–Oppenheimer approximation is based on this assumption, which allows the reduction of a mathematically intractable spectral eigenvalue problem to a set of separable spectral problems for each type of motion. According to this approximation, energy levels associated with each type of motion are proportional to the ratio of electronic mass (m_e) to the nuclei mass (M_N). This ratio, ζ , much smaller than one, is given by

$$\zeta \propto \left(\frac{m_e}{M_N} \right)^{\frac{1}{4}} \quad (1.2)$$

The electronic energy ($\Delta E_{\text{Elec.}}$) is of the order of ζ , the vibrational energy ($\Delta E_{\text{Vib.}}$) of the nuclei is of the order of ζ^2 , and the rotational energy ($\Delta E_{\text{Rot.}}$) of the molecule is of the order of ζ^4 . In quantum mechanics, states are described by wavefunctions or Hamiltonian operators, whose discrete eigenvalues define the set of energy levels and whose corresponding eigenfunctions are the basis states. Hence the total quantum wavefunction Ψ for a molecule can be written in separable form as described by

$$\Psi = \Psi_{\text{Elec.}}(r, R_0) \Psi_{\text{Vib.}}(R) \Psi_{\text{Rot.}}(\varphi_i) \quad (1.3)$$

where r is the electron coordinate, R the displacement of the nucleus from its equilibrium position R_0 , and φ_i is the Euler angles determining the orientation of molecule in space. Figure 1.3 shows the energy spectrum of matter as it is probed on a progressive finer energy scale in order to see clearly the different partition states. The fundamental and the first excited states are shown.

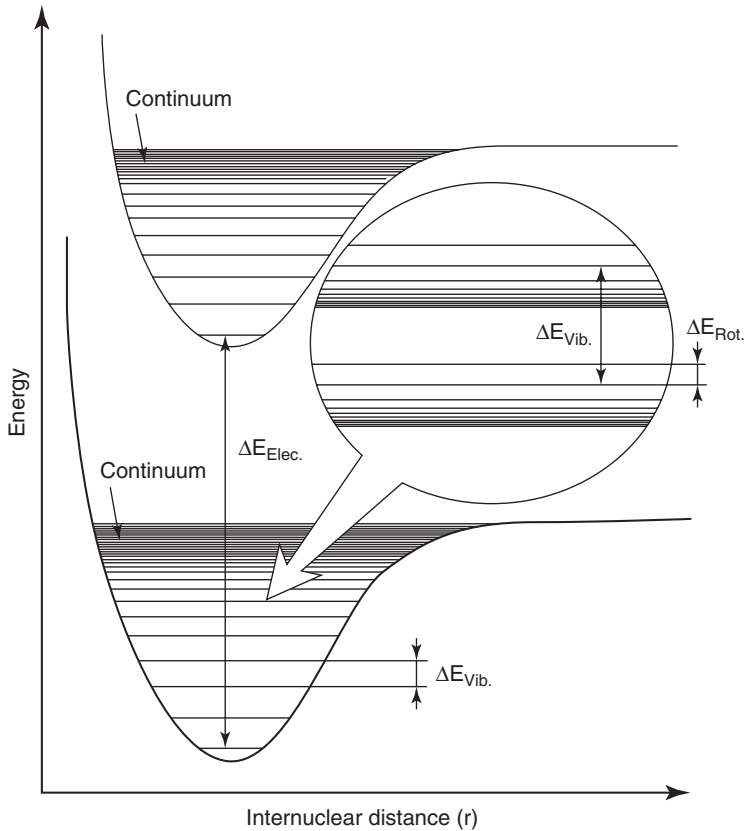


Figure 1.3 The energy spectrum of matter.

A resonance of a system can be produced by an excitation that oscillates at a frequency close to the natural frequency of the system, unlike a relaxation, which is the restoring action of a diffusive force of thermodynamic origin. Direct resonance or a one-photon process can occur in isolated intervals of the electromagnetic spectrum from ultraviolet to visible frequencies close to 10^{15} Hz (electronic oscillator), in the infrared range with frequencies close to 10^{13} Hz (vibrational modes), and in the far-infrared and microwave range with frequencies close to 10^{11} Hz (rotational modes).

1.1.2

The Complex Dielectric Permittivity

Insulating materials can be heated by applying electromagnetic energy with high frequency. The physical origin of this heating conversion lies in the ability of the electric field to induce polarization of charges within the heated product. This polarization cannot follow the extremely rapid reversals of the electric field and induce heating of the irradiated media.

The interaction between electromagnetic waves and matter is quantified by the two complex physical quantities dielectric permittivity $\tilde{\epsilon}$ and magnetic susceptibility $\tilde{\mu}$. The electric components of electromagnetic waves can induce currents of free charges (electric conduction that could be of electronic or ionic origin). It can, however, also induce local reorganization of linked charges (dipolar moments) while the magnetic component can induce structuring of magnetic moments. The local reorganization of linked and free charges is the physical origin of polarization phenomena. The storage of electromagnetic energy within the irradiated medium and the thermal conversion in relation to the frequency of the electromagnetic stimulation appear as the two main points of polarization phenomena induced by the interaction between electromagnetic waves and dielectric media. These two main points of wave–matter interactions are expressed by the complex formulation of the dielectric permittivity as described by Eq. (1.4):

$$\tilde{\epsilon} = \epsilon' - j\epsilon'' = \epsilon_0\epsilon'_r - j\epsilon_0\epsilon''_r \quad (1.4)$$

where ϵ_0 is the dielectric permittivity of vacuum, ϵ' and ϵ'' are the real and imaginary parts of the complex dielectric permittivity, and ϵ'_r and ϵ''_r are the real and imaginary parts of the relative complex dielectric permittivity, respectively. The storage of electromagnetic energy is expressed by the real part whereas the thermal conversion is proportional to the imaginary part.

✂ TOOLS More About Polar Molecules

A polar molecule has a permanent electric dipole moment. The total amounts of positive and negative charges on the molecule are equal so that the molecule is electrically neutral. However, distributions of the two kinds of charge are different, so that the positive and negative charges are centered at points separated by a distance of molecular dimensions forming an electric dipole. A dipole made up of charges $+q$ and $-q$ separated by a distance d have magnitude equal to qd . The dipole moment, usually represented by the symbol μ , is of order of magnitude 10^{-18} C (electronic charge is of the order 10^{-10} SI unit whereas d will be of the order of the molecular dimensions 10^{-10} m). The unit 10^{-18} C m is called the debye (abbreviation D).

The magnitude of the dipole moment depends on the size and symmetry of the molecule. Molecules having a center of symmetry, such as methane, carbon tetrachloride, and benzene, are apolar (zero dipole moment) whereas

molecules having no center of symmetry are polar. Table 1.2 gives the relative static dielectric permittivity or dielectric constant (very low frequency or frequency close to zero), refractive index, and dipole moment for few simple polar and apolar molecules.

Table 1.2 Relative static dielectric constant, refractive index (measured at the frequency of sodium D lines), and dipole moment for various molecules.

Molecules-	ϵ_{sr}	n_D^2	μ
<i>Apolar</i>			
<i>n</i> -Hexane C ₆ H ₁₄	1.89	1.89	–
Carbon tetrachloride CCl ₄	2.23	2.13	–
Benzene C ₆ H ₆	2.28	2.25	–
<i>Polar</i>			
Methanol CH ₃ OH	33.64	1.76	1.68
Ethanol CH ₃ CH ₂ OH	25.07	1.85	1.70
Acetone CH ₃ COCH ₃	21.20	1.84	2.95
Chlorobenzene C ₆ H ₅ Cl	5.64	2.32	1.69
Water H ₂ O	80.37	1.78	1.94

From Maxwell's theories of electromagnetic waves, it follows that the relative permittivity of a material is equal to the square of its refractive index measured at the same frequency. The refractive index given by Table 1.2 is measured at the frequency of the D lines of sodium. Hence it gives the proportion of polarizability (electronic polarizability) still effective at very high frequency (optic frequency) compared with polarizability at very low frequency given by the dielectric constant. It can be seen from Table 1.2 that the dielectric constant is equal to the square of the refractive index for apolar molecules whereas for polar molecules the difference is mainly due to the permanent dipole. In the following, the Clausius–Mossotti equation will define supplementary terms able to justify the difference between the dielectric constant and the square of the refractive index [see Eq. (1.29)].

The temperature dependence of the dielectric constant of polar molecules also differs from that of nonpolar molecules. Change of temperature has only small effect for nonpolar molecules (change of density). For polar molecules, the orientation polarization falls off rapidly with increase in temperature because the thermal motion reduces the alignment of the permanent dipoles by the electric field. In the following, we will see that it is possible to have an increasing value of dielectric permittivity with increase in temperature.

As discussed above, a molecule with a zero total charge may still have a dipole moment because molecules without center of symmetry are polar. Similarly, a molecule may have a distribution of charge which can be regarded as two equal and opposite dipoles centered at different places. Such a

distribution will have total zero total charge and zero total moment but have a quadrupole moment. Carbon disulfide, which is a linear molecule, has a quadrupole moment. Two equal and opposite quadrupole moments centered at difference places form an octupole moment. The potential due to the total charge falls off as $1/r$, that due to dipole moment as $1/r^2$, and that due to a quadrupole moment as $1/r^3$. At large distances from the distribution, the higher moments have negligible effects. However, the intermolecular distances in liquids and solids are not large compared with molecular dimensions so fairly strong interactions may arise because of higher moments.

✂ TOOLS More About Dielectrics and Insulators

An insulator is a material through which no steady conduction current can flow when it is subjected to an electric field. Consequently, an insulator can accumulate electric charge, and hence electrostatic energy. The word dielectric, especially if it is used as an adjective, covers a wide range of materials including electrolytes and even metals in optics.

If we consider a capacitor constituted by two plane-parallel plates with surface area of the plates S and thickness between plates d (S is large compared with d in order that edge effects are negligible), the vacuum capacitance is given by

$$C = \epsilon_0 \frac{S}{d} \quad (1.5)$$

If an alternating voltage $V = V_0 \exp(j\omega t)$ is applied to this capacitor, a charge $Q = CV$ appears on the electrode, in-phase with the applied voltage. The current in the external circuit is the time derivative of the charge Q and is given by

$$I = \dot{Q} = j\omega CV \quad (1.6)$$

This current is 90° out-of-phase with the applied voltage. It is a nondissipative displacement or induction current. If the volume between the electrodes is filled with a nonpolar, perfectly insulating material, the capacitor has a new capacitance; the ratio between the vacuum and filled capacitances is the relative permittivity of the material used. The new current is larger than above but it is still out-of-phase with the current. Now, if the material is either slightly conducting or polar, or both, the capacitor is no longer perfect and the current is not exactly out-of-phase with the voltage. Hence there is a component of conduction in-phase with the applied voltage. The origin of this current is motion of charges. The current is composed of a displacement current and a conduction current. The loss angle is given by

$$\tan \delta = \frac{\text{dissipative term}}{\text{capacitive term}} \quad (1.7)$$

The current is composed of two quantities, real and imaginary, so the dielectric permittivity will also have a complex form which will depend

on the types of interactions between the electromagnetic field and matter. The above discussion refers to isotropic dielectrics. Many products fall into this class but the situation is different for crystalline solids where the permittivity becomes a tensor quantity (values different according to crystallographic axis).

☛ CONCEPTS The Dielectric Properties Are Group Properties

The physical origin of polarization phenomena is the local reorganization of linked and free charges. The interaction between a dipole and an electric or magnetic field is clearly interpreted by quantum theories. In the case of an electric field, the coupling is weaker and there is such demultiplication of quantum levels that they are very close to each other. The Langevin and Boltzmann theories have to be used because the interaction energy is continuous. Due to the weak coupling between dipole and electric field, there are no quantified orientations and the study of the interaction between dipole and electric field gives more information about the surroundings of dipole than about itself. Moreover, dipoles are associated with chemical bonds and any motions of a dipole induce a correlative motion of molecular bonds, whereas motions of magnetic moment are totally independent of any molecular motions. In contrast to magnetic properties, dielectric properties are group properties and cannot be modeled by an interaction between a single dipole and electric field. A group of dipoles interacting with themselves could be considered.

The origin of confusion between the behaviors of a single dipole and a collection, or the difference between dilute and condensed phases, is the most important problem and the source of confusion within microwave athermal effects.

1.1.2.1 Effect of Real Part: Polarization and Storage of Electromagnetic Energy

The Physical Origin of Polarization Polarization phenomena are expressed by the polarization quantity \vec{P} , which gives the contribution of matter compared with vacuum. The electric field and the polarization are linked through Maxwell's equations. The constitutive equation for vacuum is given by

$$\vec{D} = \epsilon_0 \vec{E} \quad (1.8)$$

where \vec{D} is the electric displacement and \vec{E} the electric field. According to Eq. (1.8), the dielectric permittivity is the ratio of the electric displacement to the electric field. For a dielectric medium characterized by $\vec{\epsilon}$, the constitutive equation is

$$\vec{D} = \vec{\epsilon} \vec{E} = \epsilon_0 \vec{E} + \vec{P} \quad (1.9)$$

In the global formulation of Eq. (1.9), we can express the term corresponding to vacuum and given by Eq. (1.8). Then the second and complementary term defines the contribution of matter to polarization processes or polarization \vec{P} . For a material, the higher the dielectric permittivity, the greater are the Brownian ion

processes. The polarization process described by \vec{P} has its physical origin in the response of dipoles and charges to the applied field. Depending on the frequency, electromagnetic fields put one or more types of charge association into oscillation. In any material, there are various types of charge associations:

- inner or core electrons tightly bound to the nuclei
- valence electrons
- free or conduction electrons
- bound ions in crystals
- free ions as in electrolytes and nonstoichiometric ionic crystals (for example, ionic dipoles such as OH^- showing both ionic and dipolar characteristics)
- finally, the multipole (mainly the quadrupole or an antiparallel association of two dipoles).

✂ TOOLS More About Photon–Matter Interactions

Depending on the frequency, the electromagnetic field can induce one or more types of charge association under oscillation. For each configuration having its own critical frequency above which the interaction with the field becomes vanishingly small, the lower is the frequency and the more configurations are excited. Electrons of the inner atomic shells have a critical frequency of the order of the X-ray range. Consequently, an electromagnetic field of wavelength more than 10^{-10} m cannot excite any vibrations, but rather induces ionization of these atoms. There is no polarizing effect on the material which has for this frequency the same dielectric permittivity as in vacuum. For ultraviolet radiation, the energy of photons is sufficient to induce transitions of valence electrons. In the optical range, an electromagnetic field can induce distortions of inner and valence electronic shells. Polarization processes result from a dipole moment induced by distortion of electron shells and are called *electronic polarizability*. For the infrared range, electromagnetic fields induce atomic vibrations in molecules and crystals, and polarization processes result from the dipolar moment induced by distortion of nuclei positions. These polarization processes are called *atomic polarization*. In all the processes mentioned so far, the charges affected by the field can be considered to be attracted towards their central position by forces which are proportional to their displacement by linear elastic forces. This mechanical approach of electronic resonance is only an approximation, since electrons cannot be properly treated by classical mechanics. Quantitative treatments of these processes require the formalism of quantum mechanics. The two types of polarization processes described above can be connected together in distortion polarization.

The characteristic material response times for molecular reorientation are $\sim 10^{-12}$ s. Then in the microwave band, electromagnetic fields lead to rotation of polar molecules or charge redistribution: corresponding polarization processes are called *orientation polarization*.

Orienting Effect of a Static Electric Field The general problem of the orienting effect of a static electric field (orientation of polar molecules) was first considered by Debye [22, 23], Frölich [24], and, more recently, Böttcher [25, 26].

A collection of molecular dipoles in thermal equilibrium is considered. It is assumed that all the molecules are identical and they can take on any orientation. Because of thermal energy, each molecule undergoes successive collisions with the surrounding molecules. In the absence of an applied electric field, the collisions tend to maintain a perfectly isotropic statistical orientation of the molecules. This means that for each dipole pointing in one direction there is statistically a corresponding dipole pointing in the opposite direction, as illustrated in Figure 1.4.

In the presence of an applied electric field \vec{E} , the dipolar moment $\vec{\mu}$ of the molecule undergoes a torque $\vec{\Gamma}$. This torque tends to orientate the dipolar moment $\vec{\mu}$ parallel to the electric field. The corresponding potential energy (for a permanent or induced dipole) becomes minimal when the angle θ between the dipole and the electric field goes to zero. Consequently, the dipolar moment takes the same direction as the electric field. It is the same phenomenon as the orientation of a compass needle in the Earth's magnetic field. However, for molecular dipoles the thermal energy counteracts this tendency, and the system finally reaches a new statistical equilibrium which is schematically represented by Figure 1.4. In this configuration, more dipoles are pointing along the field than before. The medium becomes slightly anisotropic.

The suitability of the medium to be frozen by the electric field is given by Langevin's function resulting from statistical theories which quantify competition between the orienting effect of an electric field and the disorienting effects resulting from thermal agitation. The ratio of effective to maximal polarization versus the ratio of the potential interaction energy to the thermal agitation is shown in by Figure 1.5.

It can be seen that the Langevin function increases from 0 to 1 on increasing the strength of the electric field and/or by decreasing the temperature. The molecules tend to align with the field direction. For high values of the field, the orientation action dominates over the disorienting action induced by temperature, so that all the dipoles tend to become parallel to the applied field. The complete alignment corresponds to saturation of the induced polarization. Saturation effects

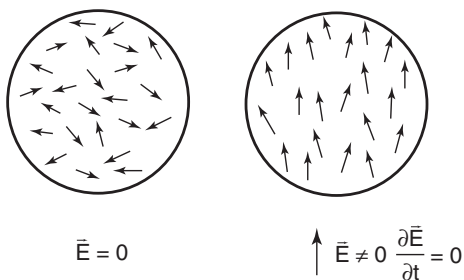


Figure 1.4 A distribution of dipoles undergoing the effect of a static electric field.

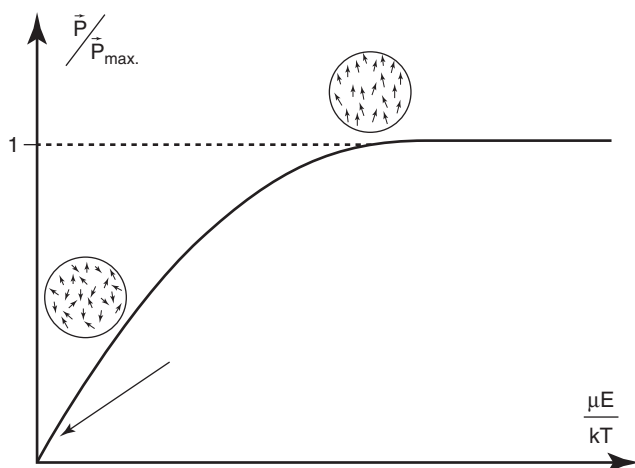


Figure 1.5 The Langevin function.

only become detectable in fields of the order of 10^7 V m^{-1} . However, because intermolecular distances are small in liquids and solids, the local field acting on a molecule and due to its neighbors may be very large, especially in strongly polar liquids (i.e., the electric field is close to 10^6 V m^{-1} at a distance of $5 \times 10^{-10} \text{ m}$ from a dipole of 1 D). However, the consequence of this remark is reduced even for the case of strongly polar liquids because the intermolecular distances are of the same order as the molecular dimensions and it is not justified to describe a molecule as a point dipole. The situation is totally different for solids and especially solid surfaces where the magnitude of the static electric field is close to the saturation value. These strong static electric fields exist independently of all external electric excitation and they are the physical origin of adsorption phenomena. In these cases, adsorption can lead to consequent freezing of molecular motions and can also induce polarization due to distortion of electronic shells. An apolar molecule can obtain a polar character due to adsorption. Free molecules without dielectric losses at the operating frequency (2.45 GHz) can reveal a capacity to heat under microwave irradiation after adsorption upon solids such as clays or alumina catalysts.

In many practical situations, field strengths are well below their saturation values. The arrow in Figure 1.5 corresponds to the usual conditions of microwave heating (no adsorption phenomena, temperature close to room temperature (25°C), and electric field strength close to 10^5 V m^{-1}). According to these results, the electric field strength commonly used in microwave heating is not sufficient to induce consequent freeze-up of media.

The calculation of the dielectric permittivity of an isotropic polar material involves the problem of the contribution of the permanent dipole to polarizability and the problem of the calculation of the local field acting at the molecular level in terms of the macroscopic field applied. Debye's model for static permittivity considers that the local field equals the external field. This assumption is only valid for gases at

low densities or dilute solutions of polar molecules in nonpolar solvents. Several workers have proposed theories with assumptions about the relation between local and external electric fields. Detailed analysis of these phenomena is beyond the scope of this section. More information can be found in Hill *et al.* [27].

1.1.2.2 Effect of Imaginary Part: Dielectric Losses

Physical Origin of Dielectric Loss The foregoing conclusions correspond to a static description or cases for which the polarization can follow perfectly the oscillation of the electric field. The electric field orientation depends on time with a frequency of 2.45 GHz (the electric field vector switches its orientation approximately every 10^{-12} s). The torque exercised by the electric field induces rotations of polar molecules, but they cannot always orient at this rate. The motions of the particles will not be sufficiently rapid to build up a time-dependent polarization $\vec{P}(t)$ that is in equilibrium with the electric field at any moment. This delay between electromagnetic stimulation and molecular response is the physical origin of the dielectric loss.

The polarization given by Eq. (1.9) becomes a complex quantity with the real part in-phase with the excitation, whereas the imaginary part have a phase lag with the excitation. This latter is the origin of the thermal conversion of electromagnetic energy within the irradiated dielectric.

◆ CONCEPTS More About Delay and Phase Lag

Matter does not respond instantaneously to stimulation induced by electromagnetic waves. In an isotropic medium, this delay can be expressed by a specific formulation of polarization given by

$$\vec{P} = \epsilon_0 \int_{-\infty}^{+\infty} \chi(t - \tau) \vec{E}(\tau) d\tau \quad (1.10)$$

because of causality principle, Eq. (1.11), where χ is the electric susceptibility, t the time, and τ the delay must be verified:

$$\chi(t - \tau) = 0, t - \tau < 0 \quad (1.11)$$

The electric susceptibility can be composed of any combination involving the dipolar, ionic, or electronic polarization processes. This formulation leads to relations between the real and imaginary parts of the complex electric susceptibility, known as the *Kramers–Kronig relations* (for more details, see [28–31]), which are very similar to the frequency relations between resistance and reactance in circuits theory (for more details, see [30]).

Consequently, after this short section upon electric susceptibility, we always shall use classical elementary models which yield to good results as can be expected from correspondence principle.

Macroscopic Theory of Dielectric Loss The main interest in dielectric theories is the frequency region where the dispersion and absorption processes occur (the dipolar polarization can no longer change fast enough to reach equilibrium with the polarization field). When a steady electric field is applied to a dielectric, the distortion polarization (electronic and vibrational modes) will be established very quickly, essentially instantaneously compared with the characteristic time of the electric field. The remaining dipolar part or orientation polarization takes time to reach the equilibrium state. Relaxation processes are probably the most important of the interactions between electric fields and matter. Debye [22, 23] extended the Langevin theory of dipole orientation in a constant field to the case of a varying field. It shows that the Boltzmann factor of the Langevin theory becomes a time-dependent weighting factor. A macroscopic description, more usable, can use an exponential law with a macroscopic relaxation time τ or the delay in the response of the medium to the electric stimulation given by

$$\vec{P}_{\text{Orientation}} = \left(\vec{P}_{\text{Total}} - \vec{P}_{\text{Distortion}} \right) \left[1 - \exp\left(-\frac{t}{\tau}\right) \right] \quad (1.12)$$

Similarly, when the electric stimulation is removed, the distortion polarization falls immediately to zero whereas the orientation polarization falls exponentially. If the electric stimulation oscillates with time (ω the angular frequency and \vec{E}_0 the electric field strength) as described by

$$\vec{E} = \vec{E}_0 \exp(j\omega t) \quad (1.13)$$

the static permittivity ε_S (frequency close to zero) and very high-frequency permittivity ε_∞ could be defined in terms of total polarization and distortion polarization:

$$\vec{P}_{\text{Total}} = \vec{P}_{\text{Distortion}} + \vec{P}_{\text{Orientation}} = (\varepsilon_S - \varepsilon_0) \vec{E} \quad (1.14)$$

$$\vec{P}_{\text{Distortion}} = (\varepsilon_\infty - \varepsilon_0) \vec{E} \quad (1.15)$$

According to the exponential law defined for the orientation polarization [Eq. (1.9)], the following differential equation could be derived:

$$\frac{d\vec{P}_{\text{Orientation}}}{dt} = \frac{(\vec{P}_{\text{Total}} - \vec{P}_{\text{Orientation}})}{\tau} = \frac{(\varepsilon_S - \varepsilon_\infty) \vec{E}_0 \exp(j\omega t) - \vec{P}_{\text{Orientation}}}{\tau} \quad (1.16)$$

The ratio of orientation polarization to electric field becomes a complex quantity. This means that the dipolar part of the polarization is out-of-phase with the field as represented by

$$\begin{aligned} \vec{P}_{\text{Total}} = \vec{P}_{\text{Orientation}} + \vec{P}_{\text{Distortion}} &= (\varepsilon_\infty - \varepsilon_0) \vec{E}_0 \exp(j\omega t) \\ &+ \frac{(\varepsilon_S - \varepsilon_0) \vec{E}_0 \exp(j\omega t)}{1 + j\omega\tau} \end{aligned} \quad (1.17)$$

Debye's Model Debye's model could be built with these assumptions and the polarization and permittivity become complex as described by

$$\tilde{\epsilon} = \epsilon' - j\epsilon'' = n^2 + \frac{\epsilon_S - n^2}{1 + j\omega\tau} \quad (1.18)$$

where n is the refractive index and τ the relaxation time. All polar substances have a characteristic time τ called the *relaxation time* (the characteristic time of reorientation of the dipolar moments in the electric field direction). The refractive index corresponding to optical frequencies or very high frequencies is given by

$$\epsilon_\infty = n^2 \quad (1.19)$$

whereas the static permittivity or permittivity for static fields correspond to ϵ_S .

The real and imaginary parts of the dielectric permittivity of Debye's model are given by

$$\epsilon' = n^2 + \frac{\epsilon_S - n^2}{1 + \omega^2\tau^2} \quad (1.20)$$

$$\epsilon'' = \frac{\epsilon_S - n^2}{1 + \omega^2\tau^2}\omega\tau \quad (1.21)$$

Changes of ϵ' and ϵ'' with frequency are shown in Figure 1.6. The frequency is displayed on a logarithmic scale. The dielectric dispersion covers a wide range of frequencies. The dielectric loss reaches its maximum given by

$$\epsilon''_{\max} = \frac{\epsilon_S - n^2}{2} \quad (1.22)$$

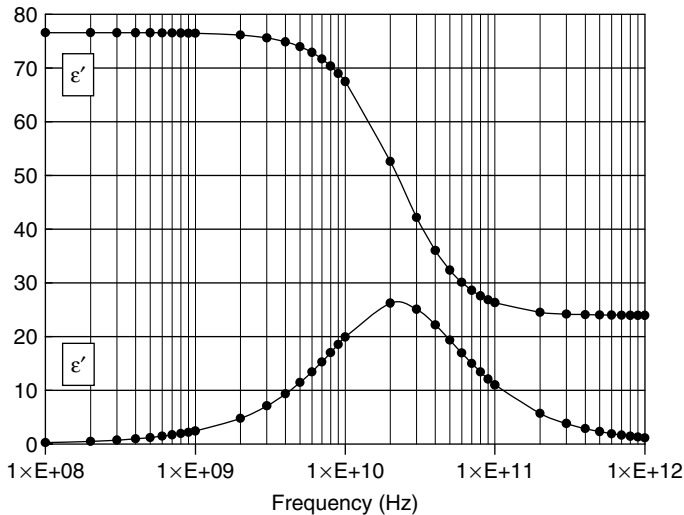


Figure 1.6 Change of the complex dielectric permittivity versus frequency. ϵ' and ϵ'' are the real and the imaginary part, respectively, of the dielectric loss for a temperature of 25 °C; dielectric parameters are $\epsilon_{Sf} = 78.2$, $\epsilon_{\infty f} = 5.5$, and $\tau = 6.8 \times 10^{-12}$ s).

at a frequency given by

$$\omega_{\max} = \frac{1}{\tau} \quad (1.23)$$

This macroscopic theory justifies the complex nature of the dielectric permittivity for media with dielectric loss. The real part of the dielectric permittivity expresses the orienting effect of an electric field with the component of polarization which follows the electric field, while the other component of the polarization undergoes a chaotic motion leading to thermal dissipation of the electromagnetic energy. This description is well adapted to gases (low density of particles). In fact, for a liquid we must take into account the effect of collisions with the surroundings and the equilibrium distribution function is no longer applicable.

☛ CONCEPTS More About the Effect of Collisions on the Distribution Function: Microscopic Theory of Dielectric Loss

The Debye theory can define a distribution function which obeys a rotational diffusion equation. Debye [22, 23] based his theory of dispersion on Einstein's theory of Brownian motion. He supposed that the rotation of a molecule due to an applied field is constantly interrupted by collisions with the neighbors, and the effect of these collisions may be described by a resistive couple proportional to the angular velocity of the molecule. This description is well adapted to liquids, but not to gases.

Molecular orientations can be specified by φ and θ . The fraction of molecules whose dipole moments lie in an element of solid angle $d\Omega$ is $f(\varphi, \theta) d\theta$. The number of representative points that pass in unit time across a unit length of θ is described by

$$\frac{\partial q}{\partial \theta} = -K \frac{\partial f(\theta)}{\partial \theta} + f(\dot{\theta}) \quad (1.24)$$

where the first term describes a diffusive process with a specific constant K and the second the effect of the electric field which sets the molecules in rotation with an average terminal angular velocity depending on the orientating couple, and on the resistive constant or damping constant of the inner friction given by

$$\zeta(\dot{\theta}) = \frac{-\partial p \vec{E} \cos \theta}{\partial \theta} \quad (1.25)$$

At equilibrium, molecular energies will be distributed according to Boltzmann's law and, finally, the general formulation which defines the factor f is given by

$$\frac{\partial f}{\partial \theta} = \frac{1}{\zeta \sin \theta} \frac{\partial}{\partial \theta} \left(kT \sin \theta \frac{\partial f}{\partial \theta} + f p E \sin^2 \theta \right) \quad (1.26)$$

The distribution function of the factor f is given by

$$f = 1 + \frac{pE \cos \theta}{kT(1 + j\omega\tau)} \quad (1.27)$$

Hence the average moment in the direction of the field is given by

$$\langle p \cos \theta \rangle = \frac{\int_0^\pi \cos \theta \left[1 + \frac{pE \cos \theta}{kT(1 + j\omega\tau)} \right] 2\pi \sin \theta d\theta}{\int_0^\pi \left[1 + \frac{pE \cos \theta}{kT(1 + j\omega\tau)} \right] 2\pi \sin \theta d\theta} \quad (1.28)$$

which can define the microscopic relaxation time that depends on the resistive force undergone by the individual molecules (for more details, see MacConnell [32]).

The general equation for complex dielectric permittivity is then given by Eq. (1.29):

$$\frac{\tilde{\epsilon}_r - 1}{\tilde{\epsilon}_r + 2} = \frac{\rho N}{3\epsilon_0 M} \left[\alpha + \frac{\mu^2}{3kT(1 + j\omega\tau)} \right] \quad (1.29)$$

where N is Avogadro's number, M is the molar mass, ρ is the specific mass, and α is the atomic polarizability. The relaxation time τ is a microscopic relaxation time that depends on the average resistive force undergone by the individual molecules. In the limit of low frequency, the Debye expression is obtained for the static permittivity, whereas in the high-frequency limit, the permittivity will fall to a value which may be written as the square of the refractive index (see Table 1.2). The first term on the left-hand side corresponds to distortion polarization, whereas the other term corresponds to orientation polarization. For apolar molecules, we obtain the well-known Clausius–Mosotti–Lorentz equation.

The Relaxation Time In the case of a spherical or nearly spherical molecule, Debye [22, 23] suggested that the molecule can be treated as a sphere (radius r) rotating in a continuous viscous medium having the viscosity η of the liquid in the bulk. The relaxation time is given by

$$\tau = \frac{8\pi \eta r^3}{2kT} \quad (1.30)$$

The relaxation time evaluated from experimental measurements is the effective time constant for the process observed even in the medium studied in case of solutions.

Owing to the incidence of the internal field factor, the relaxation time is not the value of the molecular dipole relaxation. Depending upon the internal field assumption, a variety of relations between theoretical and effective relaxation times have been defined. Relaxation times for dipole orientation at room temperature are between 10^{-10} s for small dipoles diluted in a solvent of low viscosity, and more than 10^{-4} s for large dipoles in a viscous medium such as polymers (polyethylene)

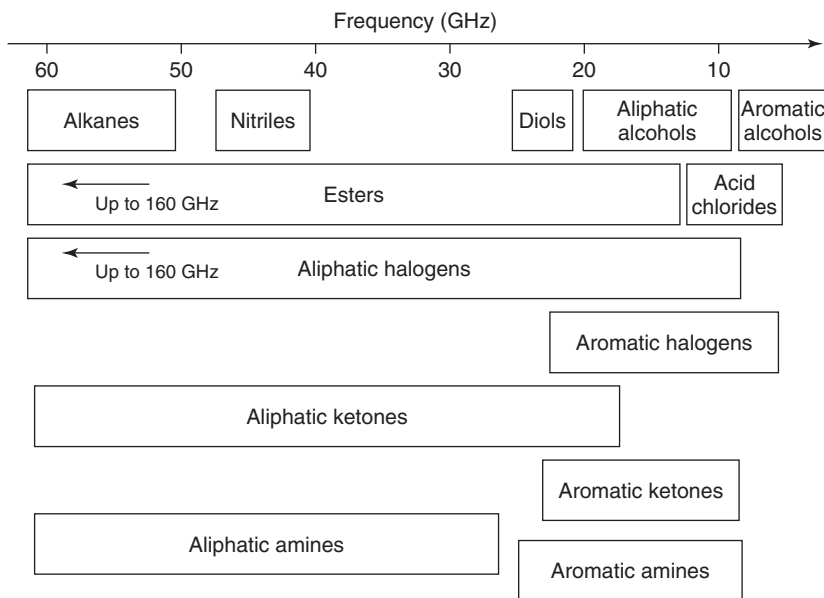


Figure 1.7 Relaxation time range for classical organic functions.

or dipole relaxations in crystals (the relaxation associated with pairs of lattice vacancies).

The relaxation times of ordinary organic molecules are close to a few picoseconds. Figure 1.7 gives the relaxation frequency range for classical organic functions: alkanes [33, 34], alcohols [35–39], alcohol ethers [40], acid chlorides [41, 42], esters [43, 44], aliphatic [45–54] and aromatic halogens [55, 56], aliphatic [57, 58] and aromatic ketones [59], nitriles [60], and aliphatic [61, 62] and aromatic amines [63].

Thus, for a frequency of 2.45 GHz, these molecules are able to follow electric field oscillations, unlike substances that are strongly associated, such as water and alcohols, and therefore exhibit dielectric loss at 2.45 GHz. Consequently the solvents which have dielectric loss are water, MeOH, EtOH, dimethylformamide (DMF), dimethyl sulfoxide (DMSO), and CH_2Cl_2 . Nonpolar solvents such as C_6H_6 , CCl_4 , and ethers have negligible dielectric loss. However, the addition of small amounts of alcohols can strongly increase the dielectric loss and microwave coupling of these solvents.

Effect of Temperature Data on the relaxation data of pure water play an important role in the discussion of the dielectric behavior of aqueous solutions. Another practical interest is the demand for dielectric reference materials suitable for use for calibrating and checking the performance of equipment for measurements of dipolar liquids. The design of microwave moisture measurement systems for food and other materials is a further aspect. The thermal and pressure dependences of the relaxation time of pure water are shown in Figure 1.8 [64].

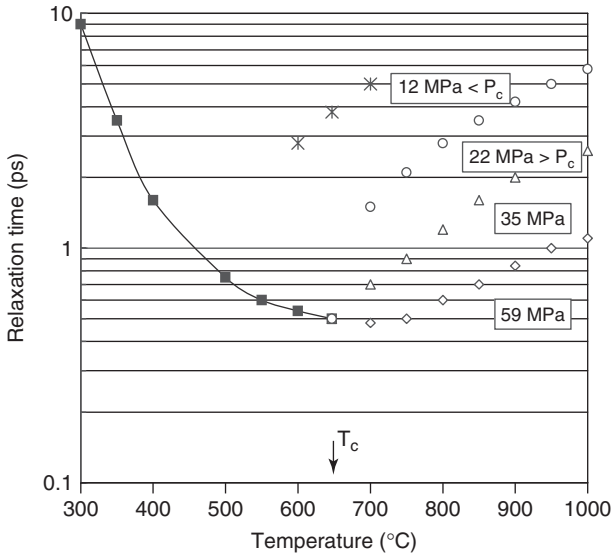


Figure 1.8 Dielectric relaxation time of pure water versus temperature and pressure. The arrow indicates the critical temperature.

The critical temperature and pressure are $T_c = 647$ K and $P_c = 22.1$ MPa. In the liquid state (continuous curve), the relaxation time decreases rapidly with increase in temperature irrespective of pressure. In the gaseous state, the relaxation time exhibits a strong pressure dependence (positive temperature dependence at constant pressure). The relaxation time jumps to a larger value at the boiling temperature when the pressure is lower than the critical pressure. More generally, the most relevant parameter at lower temperatures or higher densities is the temperature whereas at higher temperatures or lower densities it is the density. The relaxation time increases with decrease in density. The microwave field can hardly change the thermal motion of water molecules as they are rotating. This situation can be easily understood by considering the common experience that a rapidly spinning top remains standing against gravity. The orientation of the dipolar moment may be changed when the molecule loses angular momentum owing to collisions with other molecules. In the gaseous phase, the dielectric relaxation is governed by the binary collision. Recently, molecular dynamics simulations have been carried out to study the dielectric properties of supercritical water. The results showed that the assumptions for the Debye model are not valid for supercritical water because the dilute limit is avoided. Microscopically there are many degrees of freedom and all these motions are not totally decoupled from the others because the eigenstates of motion are not well known for structurally disordered matter. Dielectric measurements can only probe slow dynamics which can be described by stochastic processes and the classical Debye model could be rationalized [65, 66].

The temperature and pressure dependences for methanol are similar to those for water. Although alcohol molecules are also bonded by hydrogen bonds, the

maximum coordination is unlike that for water. The methanol molecule can form both chain and ring structures like liquid selenium [67]. The break-up of the hydrogen-bonded network is due to libration motions for water and stretching for methanol and most other alcohols.

At high densities such as under supercritical conditions, experimental relaxation times show strong deviations from the Debye model values owing to hydrogen bonding. In the gaseous phase, free molecules are responsible for the classical dielectric relaxation and molecules incorporated within the hydrogen-bonded network should be added, and the general relaxation function for supercritical fluids with hydrogen bonds is given by

$$\tilde{\varepsilon} = \varepsilon_{\infty} + (\varepsilon_S - \varepsilon_{\infty}) \left(\frac{1 - \alpha}{1 + j\omega\tau_{\text{free}}} + \frac{\alpha}{1 + j\omega\tau_{\text{bound}}} \right) \quad (1.31)$$

where α is the fraction of bound molecules and τ_{free} and τ_{bound} are the relaxation time for free molecules and bound molecules, respectively. The average relaxation time is given by

$$\tau = (1 - \alpha) \tau_{\text{free}} + \alpha \tau_{\text{bound}} \approx \tau_{\text{free}} + \alpha \tau_{\text{bound}} \text{ if } \alpha \ll 1 \quad (1.32)$$

τ_{free} can be assumed to be the binary collision time, given by

$$\tau_{\text{free}} = \frac{1}{4n\pi r_{\text{eff}}^2} \sqrt{\frac{m\pi}{k_B T}} \quad (1.33)$$

where m is the mass of the molecule and n the number density, and r_{eff} is the effective radius hard sphere diameter of the molecule equal to the intramolecular distance from Raman scattering data. In the gaseous state, α becomes small and eventually vanishes in the dilute limit whereas in the low-temperature liquid state it is replaced by an enhancement factor due to the highly correlated nature of molecular motion. The hydrogen bonding enthalpy (libration or stretching energy) can be found from

$$\tau_{\text{bound}} = \tau \exp\left(\frac{\Delta H}{k_B T}\right) \quad (1.34)$$

For the case of water, which belongs to liquids which are characterized by a discrete relaxation process in the temperature range of interest, this activation enthalpy is 4.9 kcal mol⁻¹ or hydrogen bond energy of water.

Dynamic Consequences of Dielectric Losses It is clear that for a substance with dielectric loss such as water and alcohols, the molecules do not follow perfectly the oscillations of the electric field. In the case of media without dielectric loss, and for the same reasons as in static conditions, the strength of the electric field cannot induce rotations for all polar molecules, but statistically only for a small part (less than 1%). This means that all the molecules oscillate round an average direction (precession motion), as shown in Figure 1.9.

The principal axis of the cone represents the component of the dipole under the influence of the thermal agitation. The component of the dipole in the cone is due to the field that oscillates in its polarization plane. In this way, the dipole follows

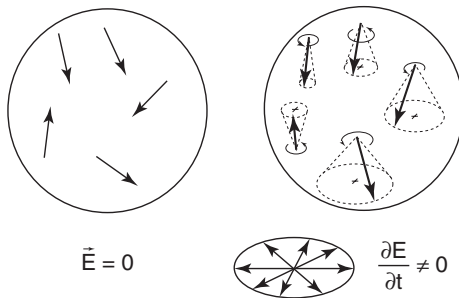


Figure 1.9 Precession motion of the dipole of a distribution of molecules undergoing irradiation by a time-dependent electric field.

a conical orbit if the Brownian motion is held up. In fact, the cone changes its direction continuously because of the Brownian motion faster than the oscillation of the electric field that leads to chaotic motion. Hence the structuring effect of an electric field is always negligible because of the value of the electric field strength, and even more for lossy media.

In condensed phases, it is well known that there are some energetic transfers between rotational and vibrational states. Indeed, molecular rotations do not actually exist in liquids; rotational states turn into vibrational states because of an increase in collisions. For liquids, the collision rate is close to 10^{30} s^{-1} . Microwave spectroscopy which studies molecular rotations only uses diluted gases in order to obtain pure rotational states with sufficient lifetimes. Broadening of rotational transitions induced by molecular collisions occurs since the values of pressure are close to a few tenths of a bar, as described in Figure 1.10.

In conclusion, for condensed phases molecular rotations have a fairly short lifetime due to collisions. Then the eventual oscillations induced by the electric field dissipate in the liquid state leading to vibration. At densities of the collisions corresponding to liquids, the frequency of the collisions become comparable to the frequency of a single rotation, and as the probability of a change in rotational state on collision is high, the time of a molecule's existence in a given state is short. According to these remarks, it is obvious that the electric field cannot induce any organization in condensed phases such as in the liquid state.

1.1.2.3 Thermal Dependence of the Dielectric Permittivity

In contrast to Eq. (1.18), Eq. (1.29) gives the frequency behavior in relation to the microscopic parameter of the studied medium (polarizability, dipolar moment, temperature, frequency of the field, etc.). Then, for a given change of the relaxation time with temperature, we can obtain the change with frequency and temperature of the dielectric properties: real and imaginary parts of the dielectric permittivity. In fact, for a given molecular system, it is better to put a formulation with $\tau_{\text{Inter}}(T)$, part of which depends on the temperature, and part totally independent of the temperature τ_{Steric} , as described by

$$\tau(T) = \tau_{\text{Steric}} + \tau_{\text{Inter}}(T) \quad (1.35)$$

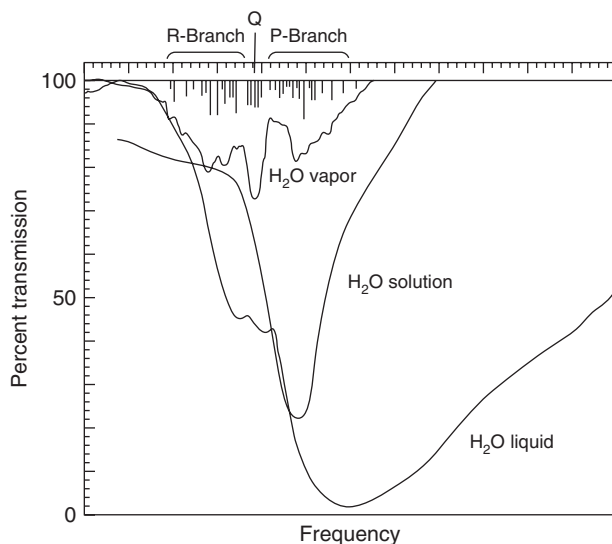


Figure 1.10 Absorption spectra for water (vapor, solution, and liquid). Above the vapor band is Mecke's rotational analysis [68, 69].

According to the value of the frequency of the field, and the relaxation time band in relation to the temperature considered, one can find the three general changes with temperature of the dielectric properties. Figure 1.11 gives the three-dimensional curves describing the dielectric properties in relation to frequency and temperature [70].

According to the value of the working frequency compared with the relaxation frequency, three general cases could be found: case 1, where the real and imaginary parts of the dielectric permittivity decrease with temperature (working frequency lower than relaxation frequency); case 2, where the real and imaginary parts of the dielectric permittivity increase with temperature (working frequency higher than relaxation frequency); and case 3, where the real and/or imaginary parts of the dielectric have a maximum (working frequency very close to relaxation frequency).

The two solvents most commonly used in microwave heating are ethanol and water. Values for water were given by Kaatze and Uhlendorf [71, 72] and values for ethanol by Chahine *et al.* [73]. Water is close to case 1 because both values decrease with temperature. In contrast, for ethanol the real part increases and the dielectric loss reaches a maximum value at 45 °C (case 2). In fact, for ethanol the working frequency is higher than the relaxation frequency at room temperature. Ethanol has a single relaxation frequency close to 1 GHz at 25 °C, and furthermore its relaxation frequency rises fairly rapidly with temperature (3 GHz at 65 °C). For water, the working frequency is smaller than the relaxation frequency at all temperatures (17 GHz at 20 °C and 53 GHz at 80 °C).

The pioneering work of Von Hippel [74] and his co-workers to obtain dielectric data for organic and inorganic materials still remains a solid basis. However, the

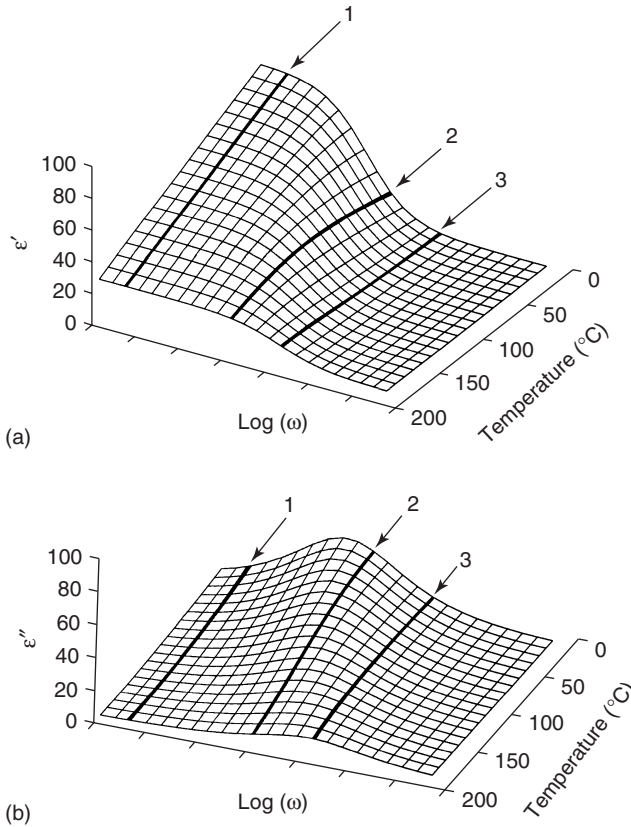


Figure 1.11 Change of the complex dielectric permittivity with frequency and temperature. ϵ' is the real part and ϵ'' the imaginary part of the dielectric loss [70].

study of dielectric permittivity as a function of temperature is less well developed, particularly for solids.

1.1.2.4 Conduction Losses

For highly conductive liquids and solids, the loss term results not only from a single relaxation term as given by Eq. (1.21) but also from a term due to ionic conductivity σ as described by

$$\epsilon'' = \frac{\epsilon_S - n^2}{1 + \omega^2 \tau^2} \omega \tau + \frac{\sigma}{\omega} \quad (1.36)$$

A conducting material can be regarded as a nonconducting dielectric with a resistance in parallel. The alternative graphical representation of plotting the logarithm of dielectric losses against the logarithm of the frequency permits the AC conductivity associated with the relaxation dipoles to be distinguished easily from the DC conductivity due to the free charges. From Eq. (1.36), two different

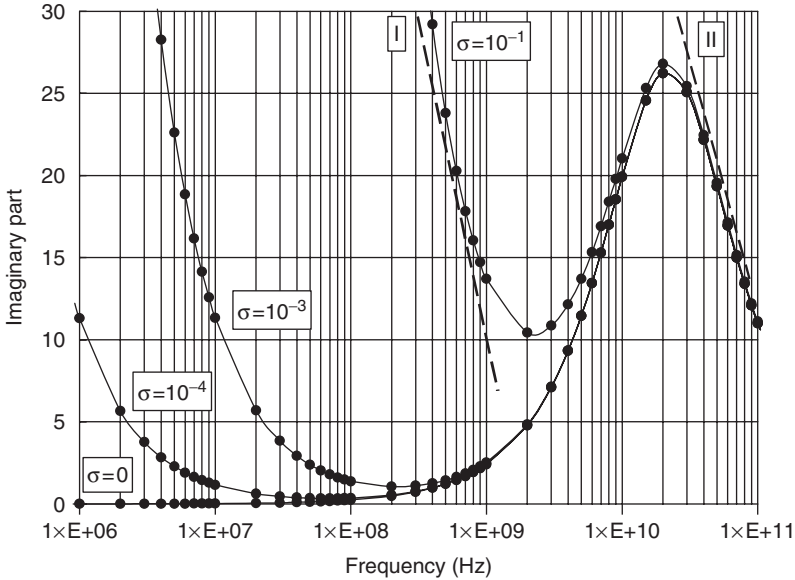


Figure 1.12 Change of dielectric losses in relation to the value of conductivity.

ranges could be defined as describe in Figure 1.12:

$$\text{for } \omega\tau \ll 1: \varepsilon'' = \frac{\sigma}{\omega}, \text{ range I} \quad (1.37)$$

$$\text{for } \omega\tau \gg 1: \varepsilon'' = \frac{\varepsilon_S - \varepsilon_\infty}{\omega\tau}, \text{ range II} \quad (1.38)$$

The second term of Eq. (1.36) is usually small with respect to the first (with typical values $\sigma = 10^{-8}$ s, $\tau = 10^{-10}$ s, $\sigma\tau = 10^{-18}$ s). This is fairly small compared with the first term, which is of the order of 10^{-11} and can be neglected.

The hydroxide ion is a typical example of ionic species showing both ionic and dipolar characteristics. For solutions containing large amounts of ionic salts, this conductive loss effect can become larger than the dipolar relaxation.

For solids, generally the conduction losses are often very small at room temperature but can change strongly with temperature. A typical example is alumina with very small dielectric losses at room temperature (close to 10^{-3}) that can reach fusion in a few minutes in a microwave cavity [75]. This effect is due to a strong increase in conduction losses associated with the thermal activation of the electrons that pass from the oxygen 2p valence band to the 3s3p conduction band. Moreover, in solids, conduction losses are generally enhanced by material defects which sharply decrease the energy gap between the valence and conduction bands. Carbon black powder exhibits high conduction losses. Hence carbon black powder can be used as a lossy impurity or additive in order to induce losses within solids exhibiting too small dielectric losses. This out-of-date trick is used by those using microwaves in heating applications. This gives an explanation of the problem met with chocolate in microwave cookers. Chocolate is constituted of lipid polymers exhibiting strong

microwave losses. Due to microwave heating, degradation of chocolate occurs very quickly and leads to carbon black production. This increases local microwave heating. Consequently, microwave heating of chocolate can quickly induce a strong burning taste.

Although the conductivity is usually a thermally activated process as given by

$$\sigma(T) = \sigma_0 \exp \left[-\frac{U}{k(T - T_0)} \right] \quad (1.39)$$

where U is the activation energy and σ_0 the conductivity at T_0 . The Joule heating within the sample cannot be extracted fast enough by conduction and/or convection so the temperature of the sample increases to a value close to the fusion temperature. The temperature dependence of solid static permittivity can lead to a strong increase in dielectric permittivity just below the melting point for the majority of crystalline or amorphous (glass) materials.

1.1.2.5 Magnetic Losses

Chemical reagents are primarily concerned with dielectric liquids or solids. However, metal oxides such as ferrites exhibit magnetic losses in the microwaves band. As for dielectrics, a complex magnetic permeability is defined as

$$\tilde{\mu} = \mu' - j\mu'' \quad (1.40)$$

The real part is the magnetic permeability whereas the imaginary part is the magnetic loss. These losses are different from hysteresis or eddy current losses because they are induced by domain wall and electron spin resonance. These materials could be placed at the position of magnetic field maxima for optimum absorption of microwave energy. Transition metal oxides such as iron, nickel, and cobalt exhibit high magnetic losses. Hence these powders can be used as lossy impurities or additives in order to induce losses within solids exhibiting too small dielectric losses.

1.2

Dielectric Properties and Molecular Behavior

1.2.1

Dielectric Properties Within a Complex Plane

1.2.1.1 Argand Diagram

Another graphical representation which is of considerable interest involves plotting the imaginary part versus the real part, or Argand diagram.

The function could be obtained by elimination of ω between Eqs. 1.20, 1.21. In the case of a simple dipole relaxation, a circle is obtained.

$$\left(\varepsilon' - \frac{\varepsilon_S - \varepsilon_\infty}{2} \right)^2 + \varepsilon''^2 = \left(\frac{\varepsilon_S - \varepsilon_\infty}{2} \right)^2 \quad (1.41)$$

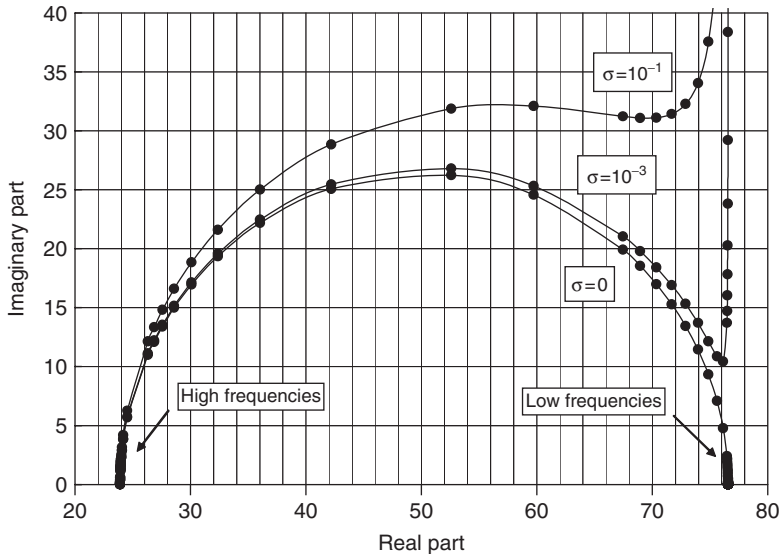


Figure 1.13 Argand diagram for different values of conductivity (S m^{-1}).

The dielectric permittivity is represented by a semicircle of radius

$$r = \frac{\varepsilon_S - \varepsilon_\infty}{2} \quad (1.42)$$

centered at

$$\varepsilon' = \frac{\varepsilon_S + \varepsilon_\infty}{2} \quad (1.43)$$

The top of this semicircle corresponds to $\tau\omega = 1$.

This plot of experimental values is a convenient graphical test of the applicability of Debye's model. The influence of the last term on the diagram shape can be seen in Figure 1.13. The higher the conductivity, the further the actual diagram departs from the Debye semicircle.

1.2.1.2 Cole–Cole Model

The Argand diagram of many polar molecules in the liquid phase is actually a semicircle as predicted by Debye's model. Typical examples are pure alcohols and symmetrical molecules such as chlorobenzene in a nonpolar solvent (alkane). Many plots deviate from this Argand plot. This deviation is usually explained by assuming that there is not just one relaxation time but a continuous distribution. Long molecules the permanent dipole moment of which is not aligned with the long molecular axis and polymers show broader dispersion curves and lower maximum losses than would be expected from Debye relationships. If the molecule is aligned with the field, only the longitudinal component of the dipole moment is active during the relaxation process. The molecule tends to rotate about a short molecular axis with a long relaxation time due to inertial and viscous forces. In contrast, if

the molecule is perpendicular to the field, the transverse component of the dipole is active and the molecule relaxes by rotating fairly quickly about its long axis because inertial and viscous forces are lower in this configuration. If the molecules are randomly oriented with respect to the field, the corresponding relaxation time is distributed between these two extreme cases which have just been considered. If $f(\tau)$ is the distribution function of the relaxation time between τ and $d\tau$, the corresponding equation for dielectric loss is

$$\varepsilon'' = \varepsilon_\infty + (\varepsilon_S - \varepsilon_\infty) \int_0^\infty \frac{f(\tau) d\tau}{1 + j\omega\tau} \quad (1.44)$$

From these observations leading to a circular arc centered below the axis, Cole and Cole [76] proposed a modified formulation of Debye's equation with h being a parameter characterizing the flattening of the diagram given by Eq. (1.45) ($h = 0$ corresponds to the classical Debye model):

$$\varepsilon'' = \varepsilon_\infty + \frac{\varepsilon_S - \varepsilon_\infty}{1 + (j\omega\tau)^{1-h}} \quad \text{with } 0 \leq h \leq 1 \quad (1.45)$$

The value of h found experimentally shows a tendency to increase with increasing number of internal degrees of freedom in the molecules and with decreasing temperature [76]. The high relaxation is associated with group rotation and molecular tumbling. Normalized skewed arc plots give evidence of an asymmetric type of distribution of the relaxation time. The value of h increases with the decrease in chain length or the distribution of the relaxation time tends towards a symmetrical distribution with decrease in chain length. The skewed arc behavior in liquids has been reported by many workers and has been explained in terms of a cooperative phenomenon and multiple relaxation processes. The molecule becomes less rigid with increase in chain length and can relax in more than one way. The different groups may rotate, in addition to the whole molecule. The former process has a smaller relaxation time compared with the latter process. The intramolecular process has similar effects to the intermolecular cooperative phenomenon observed in pure polar liquids.

1.2.1.3 Davidson–Cole Model

The above kinds of diagrams are symmetrical, and a nonsymmetrical diagram may be reasonably described by the following analytical relation proposed by Davidson and Cole [77]:

$$\varepsilon'' = \varepsilon_\infty + \frac{\varepsilon_S - \varepsilon_\infty}{(1 + j\omega\tau)^\alpha} \quad \text{with } 0 \leq \alpha \leq 1 \quad (1.46)$$

The parameter α close to 1 again reduces to Debye's model and for $\alpha < 1$ an asymmetric diagram is obtained. The Cole–Cole diagram would arise from a symmetrical distribution of relaxation times whereas the Cole–Davidson diagram would be obtained from a series of relaxation mechanisms of decreasing importance extending to the high-frequency side of the main dispersion.

1.2.1.4 Glarum's Generalization

Glarum [78] suggested a mechanism which leads to a dispersion curve barely distinguishable from the empirical skewed arc of Davidson and Cole. Glarum considered that dipole relaxation occurs by two coexisting mechanisms. Owing to lattice defects in the liquid or solid, a dipole can adapt its orientation almost instantaneously to the electric field. The presence of a hole might drastically reduce the resistance to rotation. At the same time, dipole relaxation can occur without the help of defects. Glarum considered that these two processes are independent and the general correlation function is the product of the correlation function of the two mechanisms assuming that the motion of defects is governed by a diffusion equation. Although the relaxation due to the arrival of defects is rare, a classical Debye relaxation is obtained ($\alpha = 1$). If defect diffusion is the dominant process, a circular arc is obtained with $\alpha = 0$. If the two processes coexist, $\alpha = 0.5$ is obtained. Glarum's theory was extended by Anderson and Ullman [79]. They assumed that the orientation process is a function of an environmental parameter called the *free volume*. These theories raise the possibility of deducing the fluctuation rates of environmental parameters from dielectric measurements.

1.2.1.5 Molecules with Two or More Polar Groups

Molecules constituted of a skeleton with two polar groups gives two adsorptions that overlap significantly on the frequency scale. If we use subscripts 1 and 2 for the lower and higher frequency relaxation, respectively, six parameters have to be evaluated: if the processes are quite independent, they may well be unequivocally established by the experimental data. The coexistence of two classical Debye relaxations is described by

$$\varepsilon' = \varepsilon_{\infty} + \frac{\varepsilon_S - \varepsilon_{\infty 1}}{1 + \omega^2 \tau_1^2} + \frac{\varepsilon_S - \varepsilon_{\infty 2}}{1 + \omega^2 \tau_2^2} \quad (1.47)$$

$$\varepsilon'' = \frac{\varepsilon_S - \varepsilon_{\infty 1}}{1 + \omega^2 \tau_1^2} \omega \tau_1 + \frac{\varepsilon_S - \varepsilon_{\infty 2}}{1 + \omega^2 \tau_2^2} \omega \tau_2 \quad (1.48)$$

Within a complex plane, two circles are obtained. The overlapping of these two circles depends on the vicinity of the relaxation time or relaxation frequency of the two polar groups. This assumption could be applied to more than two polar groups. Are there two isolated Debye relaxations or a distribution of relaxation time for a single relaxation process? In the latter last case, it is better to use the Cole–Cole or Davidson–Cole model. Results of permittivity measurements are often displayed by this kind of diagram. The disadvantage of these methods is that the frequency is not explicitly shown.

1.2.2

Dielectric Properties of Condensed Phases

In this section, values of the dipole moment and complex dielectric permittivity are surveyed more particularly with regard to their frequency dependence for a variety of liquid and solid systems. The varieties of dielectric phenomena which are

encountered are briefly described. They are selected to illustrate relations between dielectric data and the structure and behavior of molecular units.

In contrast to condensed phases, intermolecular interactions in gases are negligibly small. The dipole moment found in the gas phase at low pressure is usually accepted as the correct value for a particular isolated molecule. The molecular dipole moment calculated for a pure liquid using Debye's model gives values which are usually very different from those obtained from gas measurements. Intermolecular interactions in liquids produce deviations from Debye's assumptions. Short-range interactions produce a strong correlation between the individual molecules and enhance the polarization. Hydrogen bonding aligns the molecules either in chain-like structures (e.g., water and alcohols) or into anti-parallel arrangements (e.g., carboxylic acids). The atomic polarization increases and in the latter case the orientation polarization decreases by mutual cancellation of the individual molecular dipoles leading to a liquid permittivity that is smaller than values calculated for nonassociated liquids. Provided that intermolecular interactions in gases are negligibly small, the Debye model gives an adequate representation of the relation between polarization and molecular dipole moment. The dipole found in the gas phase is usually accepted as the correct value [80]. The dipole moment of chlorobenzene is 1.75 D measured in the gas phase whereas it is 1.58 D in benzene, 1.68 D in dioxane, and 1.51 D in carbon disulfide. In dilute solution, the solution's molar polarization could be expressed as the weighted sum of the molar polarization of the individual components. Significant solute–solute effects are still present even at high dilutions.

1.2.2.1 Pure Liquids: Water and Alcohols

Water and peroxides (HO–OH) represent a limiting state of such interactions. In the liquid state, water molecules associate by hydrogen bond formation. Despite its apparent complex molecular structure due to strong association water closely follows a simple Debye relaxation (at 25 °C : $\epsilon_{Sr} = 78.2$, $\epsilon_{\infty r} = 5.5$, $\tau = 6.8 \times 10^{-12}$ s, and Cole–Cole parameter $h = 0.02$). In the foregoing systems, the molecules have usually been rigid dipoles without interaction with neighbors. The situation changes significantly when hydroxyl groups are considered. Such molecules have appreciable mobility of the dipolar group. For alcohols and phenols, the hydroxyl group is able to rotate about the axis of the oxygen–carbon bond and can relax intramolecularly. However, in the liquid phase, hydroxyl groups of different molecules can interact, forming hydrogen bonds which link molecules. Alcohols such as 1- and 2-propanol lead to almost ideal semicircles in Argand plots. A skewed arc is found for halogenated alkane derivatives apart from hydrogen peroxide, the closest analog of water, and unlike the higher alcohols for which the skewed arc pattern is characteristic. Solutions of electrolytes in methanol and ethanol have shown decreased permittivity even more markedly than that observed for water. Calculations suggest that the ionic field is probably not effective beyond the first solvation layer. Maybe for the alcohols the ion solvation and its local geometric requirements lead to a proportionally larger disruption of the hydrogen-bond chains than in aqueous solutions.

1.2.2.2 Effects of Electrolytes

Relaxation processes are represented by several types of Argand diagrams such as the Debye diagram (I), Cole–Cole diagram (II), and Davidson–Cole diagram (III), or by a diagram with a few separated Debye regions. Original studies by Hasted *et al.* of aqueous solutions of salts showed only diagrams I and II [81, 82].

Since these pioneering studies, more recent experimental evidence suggests the occurrence of four types of diagram for ionic solutions. Unfortunately, experimental data are meager, and the development of dielectric measurements for these kinds of solutions is limited at present.

Recent studies have provided precise measurements of complex dielectric permittivity in a wide frequency range which covers the decimeter, centimeter, and millimeter spectral regions (7–120 GHz [83–91]). Knowledge of these data is even more crucial on going to concentrated solutions and solutions at elevated temperatures. In this case, ion–water, water–water, and ion–ion interactions become more diversified and corresponding relaxation processes become more complicated. The contribution of ionic losses causes by electric conductivity also increases, especially in the centimeter wavelength range. Increasing temperature and concentration of electrolytes induce increases in relaxation frequency or decreases in relaxation time, adding noticeable errors in determinations. Experimental evidence from measurements over a wide frequency range make it possible to describe the whole dispersion region. At high frequencies, the contribution due to electrical conductivity is smaller.

Figure 1.14 shows the change with frequency of the real and imaginary parts of aqueous NaCl solutions at high concentrations. The DC conductivity was

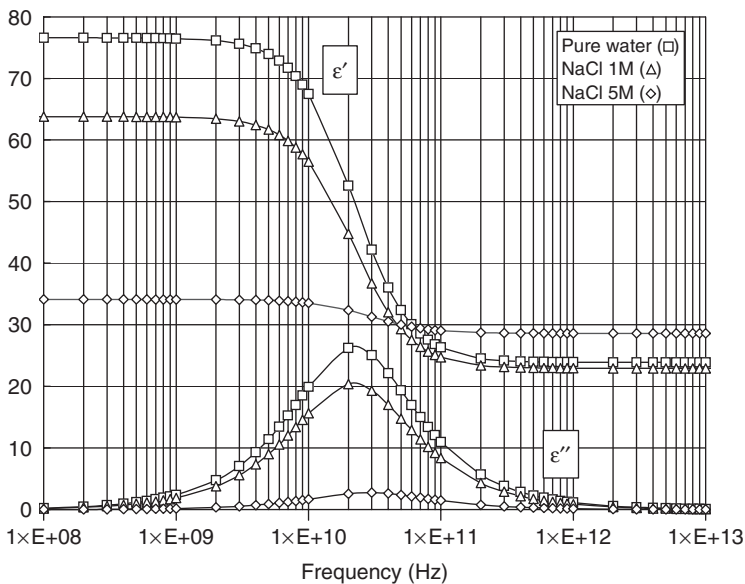


Figure 1.14 Change of real and imaginary parts of the dielectric permittivity.

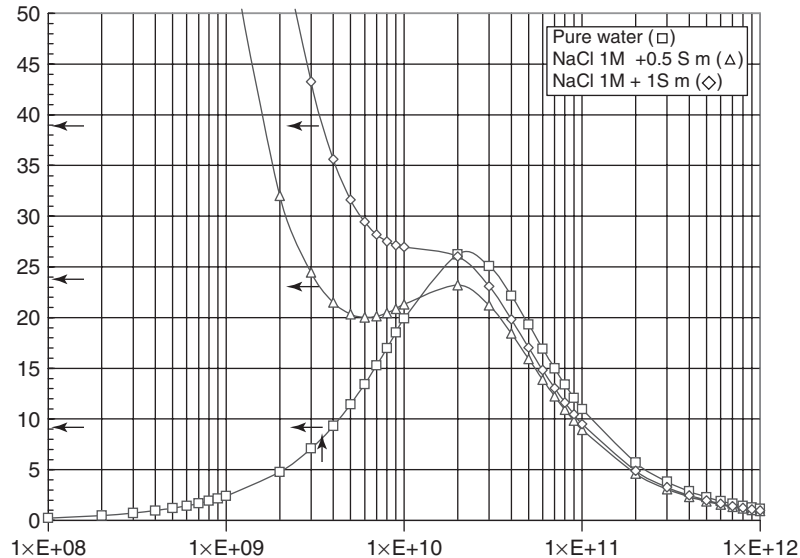


Figure 1.15 Effect of ionic conductivity on dielectric losses.

neglected by authors. They made measurements at 1 kHz using conventional methods. Addition of electrolytes usually increases the conductivity as illustrated in Figure 1.15 (arrows indicate values of dielectric losses at 2.45 GHz). No resonance or relaxation processes other than the Debye rotational diffusion of water molecules occur in the high-frequency part of the millimeter wavelength range. This indicates that ionic losses have been described by Eq. (1.36). The structural model of an electrolyte solution that reflects the difference in water molecule dynamics at various concentrations can be represented by the following scheme. In the diluted regions water molecules can be divided into molecules whose state is modified by the presence of ions (hydration shell of cations and anions) and molecules that retain all the properties of pure water (bulk water). In highly concentrated solutions, in which the bulk water is lacking, the model implies the occurrence of two states of water molecules: water molecules bound by one ion, fragment of hydration shell, and molecules shared by cations to form an ion–water cluster structure [92–102]. These different structural subsystems should be found within the dispersion region. LiCl and MgCl₂ solutions lead to two simple Debye dispersions (free and hydration shell molecules).

First, in relation to concentration, ions may associate, producing ion pairs or similar solute species of appreciable dipole moment. Such species will make their own contribution to the dielectric relaxation processes. Owing to their strong localized electric field, ions influence the solvent's molecular interactions. Addition of sodium chloride to water leads to a strong decrease in the real part of the dielectric permittivity equivalent to a temperature increase (e.g., 0.5 M sodium chloride at 0 °C has the same value as pure water at 30 °C). The value of the relaxation time

is shifted in the same sense but to a far smaller extent. The sodium chloride ions markedly change the geometric pattern of molecular interactions. According to X-ray and neutron diffraction studies, the electrostatic field neighborhood of a sodium or chloride ion is such that the interaction energy with the water–molecule dipole greatly exceeds that of a typical hydrogen bond between the solvent species. This means that an appreciable number of water molecules will be frozen around each ion, a change in molecular pattern from the liquid. The freezing of these water molecules forming a hydrate sheath around the ions means that their dipoles are not free to reorientate in the applied electric field. This causes a decrease in permittivity. This effect was quantitatively defined by Hasted *et al.* [81, 82]: for 3 M sodium chloride solution the permittivity is half the value for the pure solvent (e.g., nine water molecules immobilized per pair of sodium chloride ions). Neutral solute molecules such as ethanol noticeably increase the dielectric relaxation time of water [103–105]. This is frequently expressed by saying that the water tends to freeze to an ice-like configuration in the immediate neighborhood of the solute molecule. Many physicochemical data (e.g., entropy, partial vapor pressure, viscosity) agree in this respect. However, the situation is not a simple one, because ionized salts such as alkylammonium lead to a breakdown of the structure but nevertheless produce an increase in relaxation time. Possibly opposing effects occur: these salts are known to form a crystalline hydrate structure of the clathrate type.

Foodstuffs contain a lot of water, and many people believe that water induces microwave heating capabilities of food. According to Figure 1.15, the dielectric relaxation of water and corresponding dielectric losses are negligible for ionic solutions. Conduction losses are preponderant. Ionic species such as salts (sodium chloride) induce dielectric losses of soups and microwave heating results from ionic conduction.

1.2.2.3 Intermolecular Interactions and Complexes

Dielectric measurements of interacting solutes in inert solvents provide information regarding molecule complex formation. Some such dipoles induced by intermolecular interactions and molecular complexes in benzene solution are listed in Table 1.3. The dipole moment of the complex is a function of the relative strengths of the acid and base and the intramolecular equilibrium is described by



Stronger acid–base complexes with proton transfer induce the formation of ion-pair systems leading to high dipole moments. The OH–N interactions in acetic and chloroacetic acid with pyridine lead to an increase in polarity. Thus at least 70% ionic character is expected in the trichloroacetic acid–pyridine complex. The very high dipole moment of the picric acid–base complex shows that a predominantly ionic form exists.

Solutions of two nonpolar compounds often exhibit polar properties. Iodine solutions in benzene show a polarization greater than expected for nonpolar compounds. In most cases, the interactions involve partial electron transfer from one component to another. One component has a positive charge (donor)

Table 1.3 Dipolar moment of molecular complexes in benzene solution. Data from [27].

Components		$\mu(X - H)$	$\mu(Y)$	$\mu(H - Y)$
CH ₃ COOH	C ₅ H ₅ N	1.75	2.22	2.93
ClCH ₂ COOH	C ₅ H ₅ N	2.31	2.22	4.67
Cl ₂ CHCOOH	C ₅ H ₅ N	–	2.22	5.24
Cl ₃ CCOOH	C ₅ H ₅ N	–	2.22	7.78
CH ₃ COOH	(C ₂ H ₅) ₃ N	1.75	0.66	3.96
<i>s</i> -C ₆ H ₂ (NO ₃) ₃ OH	(<i>n</i> -Bu) ₃ N	1.75	0.78	11.4

and the other has negative charge (acceptor). In the benzene–iodine complex, partial electron transfer can be envisaged between electrons of benzene π orbitals and the lowest unfilled orbital of iodine. The degree of electron transfer determines the dipolar moment observed. Such systems, called *charge-transfer complexes*, lead to changes in other physical properties such as magnetic properties.

The relaxation times of trihalogenated esters in solution in benzene, dioxane, and carbon tetrachloride show another typical anomalous behavior, which can be explained by solute–solvent interactions. It is well known that an ester molecule is a resonance hybrid in which carbonyl assumes a positive character. This character is further accentuated by the three electron-attracting halogen groups. This positive carbonyl carbon interacts strongly with the oxygen lone-pair electrons in dioxane and π electrons of the benzene ring forming complexes with these solvents and resulting in large values of the relaxation time [54].

1.2.2.4 Intermolecular Interactions and Hydrogen Bonding

Hydrogen bonding is a form of molecular orientation involving an A–H group and an electron donor component Y; A is usually oxygen, sometimes nitrogen, and less frequently carbon. Hydrogen bond formation alters the electronic distribution within the molecules and changes the polarization and could induce a dipole moment. The polarization of *N*-substituted amides in solution increases with increase in concentration. Association into polar chains occurs with a dipole moment higher than for the monomer unit. Intermolecular hydrogen bonding occurs if the NH group is in a *trans* position with respect to the CO group. The two group dipole moments reinforce each other, producing an enhanced dipole. Solute–solvent interactions caused by hydrogen bonding can also increase the dipole moment. The increase is much larger than expected from the inductive effect alone: HBr has a dipole moment of 1.08 D in benzene solution compared with 2.85 D in dioxane solution.

1.2.2.5 What Is New About Bound Water?

Owing to the electric charge distribution of electronic orbitals, water molecules form an almost tetrahedrally structured hydrogen bond network. Computer simulation

studies [106, 107] furthermore showed that a perfect tetrahedral structure only exists at reduced water density: 84% four-coordinated molecules at $\rho = 0.75 \text{ g cm}^3$ and temperature close to 0°C according to [107]. More and more network defects appear with increase in ρ . In liquid water with $\rho = 1 \text{ g cm}^3$, all water molecules have five neighbors. Moreover, 12% of water molecules are octahedrally coordinated with six neighbors. Network defects induce smearing of the binding energy of the water molecules.

In molecular biology and food science, bound water refers to the amount of water in body tissues which are bound to macromolecules or biomolecules. The term *bound water* means hydrogen bonds stronger than in liquid water. Unfortunately, no definition exists of the energy difference between hydrogen bonds within normal and bound water. According to the literature, it is widely accepted that the dielectric spectrum of bound water should be positioned between the spectra of liquid water and ice. Kaatze [108] reviewed the evidence for bound water from implications on the dielectric properties of aqueous solutions. Broadband dielectric spectra of aqueous solutions provided experimental evidence for bound water. The extrapolated values of the static permittivity for an aqueous electrolyte solution may clearly fail compared with the predictions of mixture relations. First, this polarization decrease is due to preferential orientation around electrically charged solutes such as small multivalent ions. The permanent electric dipole moment of water molecules may be preferentially oriented in a strong electric field and may therefore be unable to follow external field changes. Such an effect of dielectric saturation likely exists also with water close to polyanions, especially when the steric order of neighboring ions or ionic groups tends to intensify the local electric field strength.

According to Kaatze [108], such water may be considered as bonded. However, no clear evidence for interaction energies exceeding the hydrogen bond energy of pure water has been found. Rather, enhanced relaxation times at low water content reflect the low concentration of hydrogen bonding sites and thus the low probability density for the formation of a new hydrogen bond.

Computer simulations by Alder and Alley [109] in 1984 showed that an ion moving in an electric field sets up a nonuniform flow. The hydrodynamic flow around an ion moving in an electric field tends to induce rotation of dipolar solvent molecules in the direction opposite to that in which they would rotate due to the field. According to Kaatze [108], the second effect could explain the polarization decrease of aqueous solutions: "the orientational polarizability of water decreases because moving ions rotate adjacent water molecules in the direction opposite to that they would rotate due to the external field. Kinetically depolarized water does not fully contribute to the electric polarization and may thus be misleadingly named bound." These new results permit the analysis of broadband dielectric spectra of aqueous solutions. The data reviewed allow bonded water to be defined and give precision to the effect of an electric field on water molecules around ions. Depolarization effects are particularly strong when water is surrounded by nonpolar components, such as in water-in-oil emulsions, vesicle solutions, and cell suspensions.

1.2.3

Dielectric Properties of Macromolecules and Polymers**1.2.3.1 Macromolecules and Polymers**

Because of their partial use in the electrical industry and because of the partial relevance of dielectric studies to questions of molecular mobility and relaxation time, extensive studies of polymer behavior have been made by dielectric methods. Only the salient feature can be outlined here.

Nonpolar polymers, such as polyethylene, polytetrafluoroethylene, and polystyrene, are especially significant for their low loss values over the widest frequency range. Polar polymers such as poly(vinyl chloride), poly(vinyl acetate), and polyacrylates show dispersion at lower frequencies than the monomeric molecules, as expected. Two or more dispersion regions are commonly observed. They are referred as α , β , and γ bands beginning with the lowest frequency dispersion. The α dispersion is broader than a Debye process. Dielectric losses have a lower maximum and persist over a wide range of frequency. Fuoss and Kirwood [110] successfully described this behavior. It is generally considered that the α dispersion is due to Brownian motion of the polymer chain whereas the β dispersion is due to oscillatory motion or intramolecular rotation of side groups.

Small molecules adopt reasonably well-defined geometry configurations and calculation of dipole moment is possible. For polymers, mobile configurations with rotations about single bonds in the chain skeleton and may occur for many side groups. The measured dipole moment is the statistical average of the mobile configurations and is proportional to the square root of the number of polar groups present in the polymer. The dipole moment μ of a polymer is usually expressed as

$$\langle \mu^2 \rangle = ng\mu_0^2 \quad (1.50)$$

where n is the number of polar groups in the chain, μ_0 is the group dipole moment of the polar unit, and g is a factor depending on the nature and degree of flexibility of the chain. Theoretical calculations of g were extensively studied by Birshtein and Ptitsyn [111] for polymers with polar groups in rigid side chains and by Marchal and Benoit [112] for polymers with polar groups within the chain backbone. In both polymers, g is a function of the energy barrier restricting rotation within the chain backbone.

The very large dipole moment of polymers provides strong intermolecular forces in solution. Atactic and isotactic polymers have different dipole moments. The dipole moment for the atactic polyvinyl isobutyl ether is 10% lower than in the isotactic form, showing that the isotactic polymer adopts a more ordered structure with group dipoles tending to align parallel to each other.

Rigid polymers possess dipole moments which are proportional to the degree of polymerization. The α -helical form of polypeptides (e.g., γ -benzyl glutamate) leads to very high dipole moments because the group dipole moments are aligned in a parallel manner. In the α -helix the carbonyl and amino groups are nearly parallel with the axis of the helix, which is stabilized by hydrogen bonding between these two groups. The calculated dipole moment for this arrangement is 3.6 D

for the peptide unit (2.3 and 1.3 D for carbonyl and amino group, respectively), in agreement with the experimental value.

1.2.3.2 Highly Functional Inorganic–Polymer Composites

Dielectric and Magnetic Performances Highly functional inorganic–polymer composite materials will soon find widespread applications, especially in microwave applications due to the flexibility in the tailoring of their electromagnetic properties associated with easy fabrication of components into desired shapes compared with their metallic or ceramic counterparts [113]. Among these materials, thermoplastic filler–polymer composites have attracted strong academic and industrial interest owing to their additional advantages of easy production and low cost. The applicability of simple component fabrication methods such as injection molding and extrusion processes is another major advantage [114]. Among the various filler materials, magnetic fillers are particularly interesting because these composites can show not only high magnetic performance but also high dielectric performance at the same time. This multifunctional behavior could be used for designed radiofrequency and microwave components such as antennas [115]. Nowadays, nanomaterials used as functional fillers are increasing in academic and industrial importance by offering unique properties compared with their counterparts employing larger particle sizes or corresponding bulk [116]. However, incorporation of nanoparticles into polymer matrices is a challenging task: dispersion of nanopowders is generally difficult owing to their high agglomeration tendency deriving from the high surface energy existing between particles [117].

Recently, several groups studying the physical and electrical properties of particulate–polymer composites have revealed the existence of interphase regions between the polymer matrices and the particles. These interphase regions consist of polymer chains that were bonded or oriented at the particle interface resulting in unique physical and electrical properties [118–120]. In this region, movement of the polymer chain is restricted owing to the interaction with the filler surface, giving the region a higher dielectric permittivity at the interface than within the bulk polymer. When the volume fraction of the interphase increases, the dielectric properties of the composite will increase. The volume fraction of the interphase is roughly a product of the interphase thickness and the area of the interface between the filler and the polymer matrix. The thickness of the interphase is affected by chemical and/or physical interactions between the filler surface and the polymer molecule. The area of the interface depends on the dispersion state of the filler in the matrix. From the dielectric behavior point of view, the metal–polymer composite system can be explained as a network of small capacitors connected in series or in parallel with each other, where the conductive particles behave as electrodes and the matrix polymer as dielectrics [121–125]. Assumption of an interphase with a slightly higher relative permittivity compared with that of the bulk at the filler surface in this system means that the relative permittivity of the dielectric between the electrodes increases slightly, thus resulting in a higher relative permittivity of the whole capacitor system. In addition, the dispersion of these surface-modified

particles is expected to be far better than that of unmodified particles. This would give a wider interface between the fillers and the matrix. Consequently, the volume fraction of the interphase with a slightly high dielectric permittivity in the composites would increase. This would also lead to a higher relative permittivity of the composites.

Nanocomposites and Clay Exfoliation Organic polymers, loaded with small amounts of montmorillonite (MMT) clay, result in polymer–clay nanocomposites (PCNs). In last two decades, PCNs have been subjected to intense industrial and academic research owing to their outstanding mechanical, thermal, chemical, and electrical properties compared with pure polymers [126–132]. MMT clay, which is also called an inorganic polymer, has a lamellar structure and excellent hydrophilic and cation-exchange properties. For its sheet dimensions, the length bandwidth can be hundreds of nanometers but the thickness is only 1 nm. MMT clay is composed of units made of two silica tetrahedral sheets centered with an alumina octahedral sheet, which is called a 2:1 phyllosilicate, and chemically it is a metal silicate. Its layers are stacked by weak dipolar or van der Waals forces, and it has both surface and edge charges. The charges on edges are easily accessible to modification, but this does not achieve much improvement in interlaminar separation. These sites represent an opportunity for the attachment of functional groups of polymers during the synthesis of PCN materials. In water or polar organic solvents, MMT clay has excellent swelling properties owing to the intercalation (absorption) of solvent molecules in the clay galleries and also the adsorption of solvent molecules on the external surfaces of its sheets. In an intercalated structure, the polymer is located in the clay galleries, expanding the clay structures but maintaining a long distance between the platelets or sheets, whereas in the case of an exfoliated structure, the original face-to-face structure of the clay platelets is destroyed and single clay sheets are randomly dispersed in the polymeric solution. Complete exfoliation of all the individual platelets is very difficult to achieve and most PCN solutions contain regions of both intercalated and exfoliated structures and their ratio depends on the polymer and clay interaction in the solutions. The structural morphology and polymer intercalation properties of the PCN films have been widely characterized by scanning and transmission electron microscopy and X-ray diffraction and Fourier transform infrared spectroscopy. The characterization of the dielectric properties of PCNs films has significant applications in integrated circuits, microelectronics, insulating devices, and membrane technology [133].

When nanocomposites are placed in an electric field they are subjected to ionic, interfacial, and dipole polarization at different time scales and length scales, making possible dielectric relaxation spectroscopy, which is uniquely suited for the study of nanocomposite dynamics. In the low-frequency range, the polymeric solutions show large dielectric dispersion due to the polymer chain segmental dynamics, ionic conduction, and electrode polarization phenomena [134–141], and these properties are governed by the solute–solvent interactions. Dielectric relaxation spectroscopy confirms the molecular dynamics in relation to the morphology of

the PCN films [142–145]. Bur and co-workers [146, 147] successfully employed dielectric relaxation spectroscopy to obtain quantitative information about the extent of clay exfoliation and its possible control in the polymer matrix in online melt PCN processes.

1.2.4

Dielectric Properties of Solids and Adsorbed Phases

1.2.4.1 Solids and Dipole Relaxation of Defects in Crystals Lattices

Molecules become locked in the solid lattice and a rigid lattice cannot make a contribution to orientational polarization. In the case of polar liquids such as water, abrupt decreases in dielectric permittivity and dielectric loss occur on freezing. Ice is transparent at 2.45 GHz. At 273 K, whereas the permittivities are closely similar (water = 87.9, ice = 91.5), the relaxation times differ by a factor 10^6 (water = 18.7×10^{-12} s, ice = 18.7×10^{-6} s). The molecular behavior in ordinary ice and features that may be relevant to a wide variety of solids were further illuminated by the systematic study of the dielectric properties of the numerous phases (ice I–VIII) formed under increasing pressure. Davidson was the first to publish an exhaustive study [148]. However, a molecule may have equilibrium positions in a solid which correspond to potential energy minima separated by a potential barrier due to interactions with neighbors. Such a molecule changes its orientation either by small elastic displacements or by acquiring sufficient energy to jump potential barriers. When an electric field is applied to a crystalline dipolar solid, polarization could occur by three mechanisms: distortion polarization, elastic displacement of dipoles from their equilibrium position, and the change in the relative orientations of dipoles.

Typical lattice defects are cation vacancies, but other types of more complicated structural defects are substitutional or interstitial ion defects. This cation vacancy behaves like a negative charge. If the temperature is high, ions are sufficiently mobile that anions could be expelled from the lattice by the Coulomb potential of the cation vacancy. Cation and anion vacancies could form a dipole oriented along one of the six crystallographic axes. This vacancy coupling is then able to induce crystalline dipoles. Similar dipoles can also appear when an ion is substituted for the host ion. A divalent atom such as calcium is substituted for a monovalent cation in alkali metal halides, releases two electrons and becomes a doubly charged ion. The new atom of calcium has an excess positive charge which couples with negative defect such as an alkali metal vacancy or an interstitial halide to create a dipole. In the following, an LiF lattice with the lattice parameter a , containing N substitutional Mg ions per unit volume, is considered. According to the Langevin model and Maxwell–Boltzmann statistics, the polarization due to the dipole defects is given by

$$P_{\text{dd}} = \frac{Na^2e^2}{6kT(1+j\omega\tau)}E \quad (1.51)$$

Li ion has been replaced by an Mg ion. This ion with its positive charge forms a dipole with a negative lithium vacancy sitting on one of the 12 nearest neighbor sites normally filled with Li ions. In the absence of an electric field, these 12 positions are strictly equivalent and the lithium vacancy hops between them, giving a zero average dipole moment for the defect considered. In the presence of an electric field, the 12 sites are no longer equivalent. Generally, the 12 sites split into three categories in relation to value of the interaction energy with the electric field. Hence the value of the dipole moment is given by

$$\mu = \frac{ae}{\sqrt{2}} \quad (1.52)$$

Finally, the complex permittivity of the substituted lattice takes the following familiar form:

$$\varepsilon'' = \varepsilon_\infty + \frac{N\mu^2}{3kT(1 + j\omega\tau)} \quad (1.53)$$

This equation describes a Debye relaxation. Magnesium- and calcium-doped lithium fluorides have a characteristic Debye relaxation diagram from which the dopant concentration and the relaxation time can be deduced. Many others crystals containing mobile lattice defects exhibit similar Debye relaxation processes. A clear understanding of the structure of color centers results from dielectric relaxation spectra. Nuclear magnetic resonance, optical, and Raman spectroscopy can be used efficiently in conjunction with dielectric spectroscopy.

1.2.4.2 Solids and Adsorbed Phases

Solid surfaces almost invariably have absorbed molecules derived from the gas or liquid medium to which the surface is exposed. The amount of such absorbed material depends upon the chemical nature of the solid surface. The absorbed layer can greatly influence the solid surface properties. The absorbed molecules may reorient by a libratory oscillation between defined orientational positions (see the subsection Orienting Effect of a Static Electric Field in Section 1.1.2.1). Such a restricted process could account for the reduced effective permittivity. The extensive occurrence of silicates (clays and soils) as catalysts in chemistry adds interest to their study

◆* CONCEPTS More About Relaxation Process Within Solids

Typical loss peaks are broader and asymmetric in solids, and frequency is often too low compared with the Debye peak. A model using the hypothesis of nearest neighbor interactions predicts a loss peak with a broader width, asymmetric shape, and lower frequency [27]. These behaviors are well suited to polymeric materials, glassy materials, and ferroelectrics. Low-temperature loss peaks typically observed for polymers need many-body interactions to be obtained. Although the present understanding of these processes is not yet sufficient to permit quantitative forecasting and dielectric properties of solids may offer insight into mechanism of many-body interactions.

1.2.5

Dielectric Properties of Interfaces and Colloidal Suspensions**1.2.5.1 Interfacial Relaxation and the Maxwell–Wagner Effect**

Dielectric absorption quantifies the energy dissipation and most systems will show energy losses from processes other than dielectric relaxation. Usually these processes are related to the DC conductivity of the medium. The corresponding loss factor of higher conductivity value persists at high frequency and even in the microwave heating range. The incidence of DC conductivity appears for fused ionic salts as a distorting feature. In addition to DC conductance loss, energy dissipation can occur by scattering of the radiation at interfacial boundaries in nonhomogeneous materials. In the visible region, the distribution of small particles of a second material (e.g., air bubbles) in an otherwise transparent medium can render it opaque. The same feature arises in dielectric media when particles are dispersed within a matrix. The general aspect of this absorption is referred as the *Maxwell–Wagner effect*.

If the dielectric material is not homogeneous but could be considered as an association of several phases with different dielectric characteristics, new relaxation processes could be observed. These relaxation processes, called *Maxwell–Wagner processes*, take place within heterogeneous dielectric materials. An arrangement constituted of a perfect dielectric without loss (organic solvent) and a lossy dielectric (aqueous solution) will behave exactly like a polar dielectric with a relaxation time that becomes greater as the conductivity becomes smaller. Such an arrangement leading to a macroscopic interface between two nonmiscible solvents could be extended to the dispersion of slightly conducting spherical particles (radius a , permittivity, and conductivity) in a nonconducting medium (dielectric permittivity equal to ε_M). In order to calculate the effective permittivity of the dispersion, consider a sphere of radius R containing n uniformly distributed particles. These particles coalesce to form a concentric sphere of radius $\sqrt[3]{na^3}$. Then, the effective dielectric permittivity of this heterogeneous medium is given by

$$\tilde{\varepsilon} = \varepsilon_\infty + \frac{\varepsilon_S - \varepsilon_\infty}{1 + j\omega\tau} \quad (1.54)$$

where the static dielectric permittivity ε_S is given by

$$\varepsilon_S = \varepsilon_M \left(1 + \frac{3na^3}{R^3} \right) \quad (1.55)$$

The system relaxes with a relaxation time given by

$$\tau = \frac{\varepsilon_P + 2\varepsilon_M}{\sigma} \quad (1.56)$$

Biological cell suspensions, under the influence of an external electric field, undergo well-pronounced dielectric relaxations in the frequency range roughly from 1 to 100 MHz [149, 150]. These dielectric dispersions, typical of highly heterogeneous colloidal systems, such as a biological cell suspensions, are due to the phenomenon of interfacial polarization, which originates when different

dielectric media, separated by a large interface, are in close contact with each other [151]. At the membrane interface an asymmetric surface charge distribution, induced by the external electric field, generates an apparent dipole moment, which is ultimately responsible for the observed dielectric relaxations.

Space-charge polarization could lead to dielectric relaxation. Accumulation of charges in the vicinity of electrodes unable to discharge the ions arriving on them can induce relaxing space-charge. The ions' behavior balances the effect of field to accumulate charge upon interfaces whereas thermal diffusion tends to avoid them (i.e., interfaces between two liquids with different dielectric permittivity and conductivity). The layer can contain charge density and is therefore equivalent to a large dipole. The sluggish dipole reversal is a relaxation process. Unlike the classical Debye model, it is impossible to separate dielectric permittivity into real and imaginary parts. An Argand diagram could be calculated and were found to be exactly semicircular and slightly flattened.

These interfacial polarization effects can explain the strong enhancement of the microwave heating rate observed by some workers with phase-transfer processes which associate an organic solvent with high lossy aqueous solutions or with dispersion of solids within nonpolar liquids. The Maxwell–Wagner loss will not appear in homogeneous liquid systems. Particularly in the case of supercooled liquids such as glasses and amorphous solids, the three loss processes, DC conductivity, Maxwell-Wagner effect, and dipolar absorption, occur simultaneously. Consequently, even if these media exhibit low dielectric loss at room temperature, slight heating will lead to a strong increase in dielectric losses related to the fusion process. For instance, an empty drinking glass placed within a domestic microwave oven can easily melt. The magnitude of this phenomenon depends on the oven power. Obviously, if a waveguide or cavity is used, an empty test-tube, a test-tube partially filled with lossy products or a test-tube filled with products without dielectric loss can lead to tube fusion. For products with a slight dielectric loss, it is better to avoid glass and to use a test-tube made of quartz or silica without dielectric loss at 2.45 GHz.

1.2.5.2 Colloids

Dielectric Properties of Colloids Colloidal solutions are the most difficult systems to measure and to analyze in dielectric terms. If the solute particle has dipole moments, the solution should show anomalous dispersion and loss at low frequencies provided that the dipole orientation involves the orientation of the whole particle. If there is a considerable difference in dielectric constants or conductivities between particles and the matrix, interfacial polarization causes dielectric loss and the frequency lies in the low-frequency range. In aqueous colloidal solutions, the presence of electrolytes even in small amounts in the water would commonly cause a sufficient conductivity difference to give interfacial polarization. In addition, there is an effect of the electric double layer at the particle surface even in the absence of an electric field. The influence of these factors must be taken into account. Errera [152] reported first results of large apparent permittivity for vanadium

pentoxide and Schwan [153]) was the first to provide experimental evidence for a strong increase in static permittivity for a polystyrene sphere suspension in water. Values of static permittivity of around 10 000 for diameters close to the micron range have been reached. The dynamics of the charge distributions within these systems lead to interesting dielectric properties which occur over a time scale range determined by various aspects of the system. The properties of colloids have been studied at radiofrequencies but very little attention has been given to their properties at microwave frequencies, probably because the charge dynamics with particles several micrometers in diameter are too slow to exhibit a significant loss at microwave frequencies.

Charged colloids typically consist of charged particles suspended in an electrolyte. Surface charges attract counterions leading to a double-layer charge. When a microwave field is applied to a charged particle, the tangential component of the electric field around the particle surface causes azimuthal transport of the double-layer ions across the particle, which results in an asymmetric charge distribution within the double layer around the particle. This charge redistribution induces a change in the dipole strength, leading to a resultant electric field around the particle which opposes the applied field [152–154]. O'Brien [155] showed that the flow of counterions results in a high-frequency, low-amplitude relaxation with relaxation time τ_1 given by

$$\tau_1 \approx \frac{1}{\kappa^2 D} \quad (1.57)$$

where κ is the reciprocal of the double-layer thickness and D is the ion diffusivity [154]. After this charge redistribution of the double layer, a slower relaxation process takes place within the electrolyte. The low-frequency relaxation time τ_2 is given by

$$\tau_2 = \frac{R^2}{D} \quad (1.58)$$

where R is the radius of the particle. The size dependence of this dissipative process is of particular interest for microwave heating. Hussain *et al.* [156] showed that polystyrene particles with surface charge resulting from sulfate groups suspended in pure distilled water (diameter between 20 and 200 nm) exhibited relaxation beyond 10 GHz associated with the dipolar relaxation of water. The dielectric permittivity and dielectric loss induced by colloids over this region are slightly lower than those produced by water. Dielectric losses are in agreement with the additional DC static conductivity of the colloid given by Eq. (1.36). Bonincontro and Cametti [157] and Buchner *et al.* [158] described how dielectric measurements can be used to obtain information about electric polarization mechanisms occurring at different time scales for ionic and nonionic micellar solutions, liposomes, and biological cell suspensions. Jönsson *et al.* [159] discussed the effect of interparticle dipolar interaction on the magnetic relaxation for magnetic nanoparticles. It seems that superparamagnetic behavior could be replaced by spin-glass-like dynamics for those systems.

Flocculation Processes The separation of the particulate phase from a suspension is an important unit operation in many industrial and environmental processes. To achieve effective separation, a prior flocculation process is often necessary. The agglomeration of particles into larger aggregates increases the settling velocity [160] of the particulate phase and lowers the specific resistance to filtration [161, 162]. Flocculation is commonly induced by the adsorption of synthetic polymers on particle surfaces. Depending on the characteristics of the polymer and the particle, the adsorption will generally facilitate flocculation through one of three mechanisms: charge neutralization caused by the evenly distributed adsorption of a low molecular weight polymer [163], patch flocculation caused by mosaic-like adsorption of a highly charged medium molecular weight polymer, resulting in a patch-like charge inversion [164], or bridging caused by the adsorption of a high molecular weight polymer on more than one particle [165]. Flocculation has been the subject of several studies, both theoretical [160, 163, 164, 166–169] and experimental [170–173]. Describing the process in generalized terms is complicated by the complex kinetics of polymer mixing, polymer–particle collisions, polymer adsorption, polymer re-configuration, particle–particle collisions, and particle–particle breakup [174]. As the interparticle forces responsible for the particle aggregation are influenced by the adsorbed polymer and its configuration on the particle surface, evaluating these forces is not easy and experimental methods for monitoring the process on-line are needed.

As many industrial processes involve suspensions of high solids content, methods for the characterization of flocculation in nondilute suspensions are of interest, from both industrial and research viewpoints. The use of rheological measurements to assess the state of flocculation has been investigated previously in sludges, but it was found difficult to obtain a direct correlation between the rheological data and optimum polymer dosage [175].

A method that has been used extensively to characterize colloidal suspensions is dielectric spectroscopy (DS) [176–181]. The frequency-dependent permittivity of a suspension can be measured. In the kilohertz range, a dispersion of the permittivity is found in colloidal suspensions. At low frequencies, the permittivity reaches values that can be several orders of magnitude higher than at higher frequencies. This phenomenon is caused by a relaxation process, termed α relaxation. The mechanism responsible for this relaxation is the occurrence of a diffusion current across the diffuse part of the electrical double layer. The ionic diffusion arises as an effect of the difference in the field-induced ionic fluxes in and out of the double layer due to different concentrations in the bulk and in the double layer [182]. At low frequencies, the time available for concentration polarization is sufficient to create a dipole, which results in an increase in permittivity. At high frequencies, however, the time available for ionic diffusion is insufficient and no such effect is evident. From the α relaxation, information on both particle charge and size can be extracted [183]; moreover, the measurements can be made over a wide particle concentration range [181]. Furthermore, Genz *et al.* used DS to investigate the shear-dependent deflocculation of aggregates of carbon black particles [184], finding that changes in dielectric dispersion could be attributed to the deflocculation process. The use of

impedance spectroscopy to study the coagulation of blood has been reported [185, 186] and the overall capacitance of the sample was found to increase as the blood coagulated. The fact that DS and related techniques have previously been used to obtain information on processes involving structural changes further justifies their use in characterizing flocculation processes. The use of DS to study the flocculation of polystyrene particles with poly(DADMAC) [poly(diallyldimethylammonium chloride)] was investigated by Christensen and co-workers [187, 188]. The dielectric dispersion of the suspension, measured at various polymer dosages, was modeled using the Cole–Cole model. More recently, Christensen *et al.* [189] used DS as a method for evaluating the flocculation of model core–shell particles. Particles with varying shell thickness were synthesized and flocculated using two highly charged poly(DADMAC) polymers. In addition to the measurement of the dielectric dispersion, the flocculation process was characterized using a photometric dispersion analyzer and measurements of electrophoretic mobility as reference methods. Hydrophobically modified poly(acrylic acid) polymers were also used as model macromolecules and coagulated with barium ions [190]. The potential of using DS to monitor the coagulation of hydrophobically modified poly(acrylic acid) polymers was investigated. The relaxation time (τ) obtained from DS was observed to increase markedly as coagulation of the polymers was facilitated by the added barium. The use of τ as an indicator of coagulation therefore seems appropriate.

Thus, whereas most existing methods provide information on only one parameter, such as size or charge, DS has the potential to monitor both size and charge even at high particle concentrations. This makes DS a promising method for evaluating flocculation processes and a powerful tool in characterizing colloids and colloidal processes

Particle Shape and Electrokinetic Behavior The response of nonspherical charged colloids to electric fields involves a complex set of processes acting in different frequency ranges and determining, at least in principle, an electrokinetic behavior differing from that of spherical particles. Recent theoretical and experimental advances in this area have allowed the determination of the extent to which the shape affects the behavior in a measurable way. Whereas electrophoretic mobility, both as a response to static fields and through electroacoustic measurements, is fairly insensitive to the particle shape, dielectric permittivity spectra can be significantly modified. This is particularly true for rod-like particles, where the α relaxation frequency depends strongly on the orientation of the particles. The description of model particles, made stronger by recent theoretical advances and recent experiments on disk-shaped and rod-like particles, now has the potential to tackle better the behavior of more complex systems, such as DNA, for which an important body of recent observations is already available. Specific for dispersions of nonspherical colloids are those electro-optic properties that have no counterpart in suspensions of spherical particles. Some electro-optic spectral measurements, such as electric birefringence, electric dichroism, and electric light scattering, also depend on the same phenomena occurring in and around the electric double layer of the particles that also determine the dielectric spectra. However, the electro-optic

response depends on the polarization of the electric double layer in a different way, being sensitive to its anisotropy rather than to its mean value. The spectral sensitivities of DS and electro-optic spectroscopy also differ, the former being mostly sensitive to the low-frequency α relaxation, whereas the latter is strongly determined by the contribution of molecular weight to the polarizability. Recent advances in this field have shown that the electro-optic response at low frequency is also affected by electrohydrodynamic flows having a nonlinear dependence on E . Such flows might be responsible for the repeatedly reported anomalous orientation of rod-like and disk-shaped particles. These phenomena have an intimate connection with the recently developing field of nonlinear electrokinetics, still largely to be described. Recently, Jiménez and Bellini [191] published a review of this open area.

1.3

Conclusion

Dielectric or insulating materials can be heated by applying electromagnetic energy with high frequency. The physical origin of this heating conversion lies in the ability of the electric field to induce polarization of charges within the heated product. This polarization cannot follow the extremely rapid reversals of the electric field and induce heating of the irradiated media. The interaction between electromagnetic waves and matter is quantified by the two complex physical quantities dielectric permittivity and magnetic susceptibility. The electric components of electromagnetic waves can induce currents of free charges (electric conduction that could be of electronic or ionic origin). It can, however, also induce local reorganization of linked charges (dipolar moments) whereas the magnetic component can induce structuring of magnetic moments. The local reorganization of linked and free charges is the physical origin of polarization phenomena. The storage of electromagnetic energy within the irradiated medium and the thermal conversion in relation to the frequency of the electromagnetic stimulation appear as the two main points of polarization phenomena induced by the interaction between electromagnetic waves and dielectric media. These two main points of wave–matter interactions are expressed by the complex formulation of the dielectric permittivity and magnetic susceptibility.

The physical origin of polarization phenomena is the local reorganization of linked and free charges. The interaction between a dipole and an electric or magnetic field is clearly interpreted by quantum theories. In the case of an electric field, the coupling is weaker and there is such demultiplication of quantum levels that they are very close to each other. The Langevin and Boltzmann theories have to be used because the interaction energy is continuous. Owing to the weak coupling between dipole and electric field there are no quantified orientations and the study of interactions between a dipole and an electric field gives more information about the surroundings of the dipole than about itself. Moreover, dipoles are associated with chemical bonds and any motion of a dipole induces a correlative motion of molecular bonds, whereas motions of magnetic moment are totally independent

of any molecular motions. In contrast to magnetic properties, dielectric properties are group properties and cannot be modeled by an interaction between a single dipole and an electric field. A group of dipoles interacting with themselves could be considered. The origin of the confusion between the behaviors of a single dipole and a collection, or the difference between dilute and condensed phases, is the most important problem and the source of confusion about microwave athermal effects.

Consequently, dielectric properties could be used to deduce the structures and behavior of molecular systems in terms of intermolecular interactions even for pure products or solutions. Recent broadband dielectric spectra of aqueous solutions have given precision to the effect of an electric field upon water molecules surrounded by nonpolar components, such water-in-oil emulsions, vesicle solutions, and cell suspensions.

All solids contain mobile lattice defects which exhibit the Debye relaxation process. A clear understanding of the structure of color centers and defects has resulted from dielectric relaxation spectra. Nuclear magnetic resonance, optical, and Raman spectroscopy can be used efficiently in conjunction with DS.

Colloidal solutions and suspensions are the most difficult systems to measure and to analyze in dielectric terms. If the solute particle has dipole moments, the solution should show anomalous dispersion and loss at low frequencies provided that the dipole orientation involves orientation of the whole particle. If there is a considerable difference in dielectric constant or conductivity between particles and the matrix, interfacial polarization causes dielectric loss and the frequency is in the low-frequency range. In aqueous colloidal solutions, the presence of electrolytes even in small amounts in the water would commonly cause a sufficient conductivity difference to give interfacial polarization. In addition, there is an effect of the electric double layer at the particle surface even in the absence of an electric field. The influence of these factors must be taken into account. Recently, the potential of DS to monitor the coagulation and flocculation of colloidal suspensions has been investigated. The use of the relaxation time as an indicator of coagulation therefore seems appropriate.

In conclusion, dielectric properties within microwave bands have grown tremendously in stature over the past few years and are now being widely used to monitor a great variety of physicochemical media.

References

1. Macquer, P. (1766) *Dictionnaire de Chymie Contenant la Théorie et la Pratique de Cette Science*, Vol. II, Lacombe, Paris, p. 503.
2. Hull, A.W. (1921) *Phys. Rev.*, **18**, 31.
3. Hull, A.W. (1921) *AIEE J.*, **40**, 715–718.
4. Hollman, H. (1935) *Physics and Technology of Ultrashort Waves*. This classic reference had much more influence on wartime technological developments in the UK and the USA than in Germany. US Patent 2,123,728.
5. Anonymous (1946) *Electronics*, **19** (11), 178.
6. Anonymous (1946) *Elec. Eng.*, **65** (12), 591.
7. Decareau, R.V. and Peterson, R.A. (1986) *Microwave Processing and*

- Engineering, VCH Verlag GmbH, Weinheim.
8. Spencer, P.L. (1950) US Patent 2,495,429; Spencer, P.L. (1952), US Patent 2,593,067; Spencer, P.L. (1952) US Patent 2,605,383.
 9. Proctor, B.E. and Goldblith, S.A. (1951) *Adv. Food Res.*, **3**, 120–196.
 10. Jackson, S.M., Rickter, S.L., and Chichester, C.O. (1957) *Food Technol.*, **11** (9), 468–470.
 11. Copson, D.A. and Decareau, R.V. (1957) *Food Res.*, **22**, 402–403.
 12. Copson, D.A. (1954) *Food Technol.*, **8** (9), 397–399.
 13. Copson, D.A. (1956) *IRE Trans., PGME-4*, 27–35.
 14. Copson, D.A. (1958) *Food Technol.*, **12** (6), 270–272.
 15. Copson, D.A. (1975) *Microwave Heating*, 2nd edn., AVI Publishing, Westport, CT.
 16. Copson, D.A. and Krajewski, E.Z. (1958) US Patent 3,020,645.
 17. Lipoma, S.P. and Watkins, H.E., (1968) US Patent 3,365,301.
 18. O'Meara, J.P. (1973) *J. Microwave Power*, **8**, 167–172.
 19. Smith, D.P. (1969) *Microwave Energy Appl. Newsl.*, **2** (3), 9–10.
 20. Decareau, R.V. (1985) *Microwaves in the Food Processing Industry*, Academic Press, New York.
 21. Lee, T.H. (2004) *Planar Microwave Engineering*, Cambridge University Press, Cambridge.
 22. Debye, P. (1913) *The Collected Papers of Peter J. W. Debye*, Interscience, New York.
 23. Debye, P. (1947) *Polar Molecules*, Dover Publications, New York.
 24. Frölich, H. (1958) *Theory of Dielectrics: Dielectric Constant and Dielectric Loss*, Clarendon Press, Oxford.
 25. Böttcher, C.J. (1973) *Theory of Electric Polarization: Dielectrics in Static Fields*, Vol. 1, Elsevier, Amsterdam.
 26. Böttcher, C.J. (1978) *Theory of Electric Polarization: Dielectrics in Time-Dependent Fields*, Vol. 2, Elsevier, Amsterdam.
 27. Hill, N.E., Vaughan, W.E., Price, A.H., and Davies, M. (1969) *Dielectric Properties and Molecular Behaviour*, Van Nostrand Reinhold, London.
 28. Landau, L.D. and Lifshitz, E.M. (1960) *Electrodynamics of Continuous Media* (translated by Sykes, J.B. and Bell, J.S.), Pergamon Press, Oxford.
 29. Jackson, J.D. (1975) *Classical Electrodynamics*, 2nd edn., John Wiley & Sons, Inc., New York.
 30. Ramo, S., Whinnery, J.R., and Van Duzer, T. (1984) *Fields and Waves in Communication*, 2nd edn., John Wiley & Sons, Inc., New York.
 31. Coelho, R. (1978) *Physics of Dielectrics for the Engineer*, Fundamental Studies in Engineering, Vol. 1, Elsevier, Amsterdam.
 32. MacConnell, J. (1980) *Rotational Brownian Motion and Dielectric Theory*, Academic Press, London.
 33. Göttmann, O. and Stumper, U. (1973) *Chem. Phys. Lett.*, **22** (2), 387–389.
 34. Pardee, G.W.F. (1970) *Trans. Faraday Soc.*, **66**, 2699–2709.
 35. Sharma, R.S. and Sofi, G.Q. (1976) *Acta Licencia Indica*, **2** (4), 364–368.
 36. Crossley, J. (1979) *Adv. Mol. Relax. Interact. Process.*, **14**, 115–120.
 37. Koszoris, L. and Masszi, G. (1982) *Acta Biochim. Biophys. Acad. Sci. Hung.*, **17** (3–4), 237–249.
 38. Hanna, F.F. and Bishai, A.M. (1976) *Z. Phys. Chem. (Leipzig)*, **257** (6), 1241–1248.
 39. Hanna, F.F. and Bishai, A.M. (1977) *Z. Phys. Chem. (Leipzig)*, **258** (4), 609–614.
 40. Purohit, H.D. and Sengwa, R.J. (1991) *Bull. Chem. Soc. Jpn.*, **64** (6), 2030–2031.
 41. Purohit, H.D. and Sharma, H.S. (1973) *Indian J. Pure Appl. Phys.*, **11**, 664–665.
 42. Purohit, H.D. and Sharma, H.S. (1977) *Bull. Chem. Soc. Jpn.*, **50** (10), 2606–2608.
 43. Koga, Y., Takahashi, H., and Higasi, K. (1974) *Bull. Chem. Soc. Jpn.*, **47** (1), 84–87.
 44. Srivastava, G.P., Mathur, P.C., and Krishna, M. (1972) *Can. J. Phys.*, **50**, 1449–1452.

45. Anthony, A.A. and Smyth, C.P. (1964) *J. Am. Chem. Soc.*, **86**, 152–158.
46. Chandra, S. and Prakash, J. (1971) *J. Chem. Phys.*, **54** (12), 5366–5371.
47. Crossley, J. and Smyth, C.P. (1969) *J. Am. Chem. Soc.*, **91** (10), 2482–2487.
48. Srivastava, S.K. and Srivastava, S.L. (1977) *Indian J. Phys.*, **51B**, 26–32.
49. Roy, S.K., Sengupta, K., and Roy, S.B. (1977) *Indian J. Phys.*, **51B**, 42–49.
50. Purohit, H., Kumar, S., and Vyas, A.D. (1980) *Adv. Mol. Relax. Interact. Process.*, **16**, 166–173.
51. Purohit, H., Sharma, H.S., and Vyas, A.D. (1975) *Bull. Chem. Soc. Jpn.*, **48** (10), 2785–2788.
52. Gottman, O., and Stumpre, U. (1973) *Chem. Phys. Lett.*, **22** (2), 387–389.
53. Purohit, H.D., and Sharma, H.S. (1973) *J. of Pure and Applied Physics.*, **11**, 664–665.
54. Purohit, H.D., Sharma, H.S., and Vyas, A.D. (1977) *Can. J. Phys.*, **55**, 1902–1905.
55. Arrawatia, M.L., Sisodia, M.L., Gupta, P.C., and Kabra, S.C. (1991) *J. Chem. Soc., Faraday Trans. 2*, **77**, 169–180.
56. Klages, G. (1988) *Z. Naturforsch.*, **43a**, 1–13.
57. Crossley, J. (1972) *J. Chem. Phys.*, **56** (6), 2549–2552.
58. Madan, M.P. (1975) *Can. J. Phys.*, **53**, 23–27.
59. Farmer, D.B., Mountain, P.F., and Walker, S. (1973) *J. Phys. Chem.*, **77** (5), 714–717.
60. Firman, P., Marchetti, A., Xu, M., Eyring, E.M., and Petrucci, S. (1991) *J. Phys. Chem.*, **95**, 7055–7061.
61. Arcega Solsona, F.J. and Fornies-Marquina, J.M. (1982) *J. Phys. D: Appl. Phys.*, **15**, 1783–1793.
62. Sengupta, K., Roy, S.K., and Roy, S.B. (1977) *Indian J. Phys.*, **51B**, 34–41.
63. Vij, J.K., Krishan, I., and Srivastana, K.K. (1973) *Bull. Chem. Soc. Jpn.*, **46**, 17–20.
64. Yao, M. and Hiejima, Y. (2002) *J. Mol. Liq.*, **96–97**, 207–220.
65. Skaf, M.S. and Laria, D. (2000) *J. Chem. Phys.*, **113**, 3499–3502.
66. Yang, C.N. and Kim, H.J. (2000) *J. Chem. Phys.*, **113**, 6025–6032.
67. Narten, A.H. and Habenschuss, A. (1984) *J. Chem. Phys.*, **80**, 3387–3393.
68. Kinsey, E.L. and Ellis, J.W. (1937) *Phys. Rev.*, **51**, 1074–1078.
69. West, W. (1939) *J. Chem. Phys.*, **7**, 795–801.
70. Stuerger, D. and Gaillard, P. (1996) *J. Microwave Power Electromagn. Energy*, **31**, 101–113.
71. Kaatze, U. and Uhlendorf, V. (1981) *Z. Phys. Chem. Neue Folge*, **126**, 151–165.
72. Kaatze, U. (1989) *J. Chem. Eng. Data*, **34**, 371–374.
73. Chahine, R., Bose, T.K., Akyel, C., and Bosisio, R.G. (1984) *J. Microwave Power Electromagn. Energy*, **19**, 127–134.
74. Von Hippel, A.R. (1954) *Dielectric Materials and Applications*, MIT Press, Cambridge, MA.
75. Berteaud, A.J. and Badot, J.C. (1976) *J. Microwave Power Electromagn. Energy*, **11**, 315–318.
76. Cole, K.S. and Cole, R.H. (1949) *J. Chem. Phys.*, **9**, 341–345.
77. Davidson, D.W. and Cole, R.H. (1951) *J. Chem. Phys.*, **18**, 1417–1422.
78. Glarum, S.H. (1960) *J. Chem. Phys.*, **33**, 369.
79. Anderson, J.E. and Ullman, R. (1967) *J. Chem. Phys.*, **47**, 2178–2184.
80. McClellan, A.L. (1967) *Tables of Experimental Dipole Moments*, W.H. Freeman, San Francisco, CA.
81. Hasted, J.B., Ritson, D.M., and Collie, C.H. (1948) *J. Chem. Phys.*, **16** (1), 1–11.
82. Hasted, J.B., Ritson, D.M., and Collie, C.H. (1948) *J. Chem. Phys.*, **16** (1), 12–21.
83. Lyashchenko, A.K. and Zasetky, A.Y. (1998) *J. Mol. Liq.*, **77**, 61–75.
84. Asheko, A.A. and Nemchenko, K.E. (2003) *J. Mol. Liq.*, **105** (2–3), 295–298.
85. Lileev, A.S., Filimonova, Z.A., and Lyashchenko, A.K. (2003) *J. Mol. Liq.*, **103–104**, 299–308.
86. Barthel, J. (1995) *J. Mol. Liq.*, **65/66**, 177–185.
87. Nakahara, M. and Wakai, C. (1995) *J. Mol. Liq.*, **65/66**, 149–155.
88. Frood, D.G. and Gallagher, T.J. (1996) *J. Mol. Liq.*, **69**, 183–200.

89. Barthel, J., Buchner, R., Eberspächer, P.N., Münsterer, M., Stauber, J., and Wurn, B. (1998) *J. Mol. Liq.*, **78**, 83–109.
90. Tassaing, T., Danten, Y., and Besnard, M. (2002) *J. Mol. Liq.*, **101** (1–3), 149–158.
91. Vij, J.K., Simpson, D.R.J., and Panarina, O.E. (2004) *J. Mol. Liq.*, **112**, 125–135.
92. Sutmann, G. and Vallauri, R. (2002) *J. Mol. Liq.*, **98–99**, 213–224.
93. Chialvo, A.A., Cummings, P.T., and Simonson, J.M. (2003) *J. Mol. Liq.*, **103–104**, 235–248.
94. Geiger, A., Kleene, M., Paschek, D., and Rehtanz, A. (2003) *J. Mol. Liq.*, **106** (2–3), 131–146.
95. Malenkov, G.G., Tytik, D.L., and Zheligovskaya, E.A. (2003) *J. Mol. Liq.*, **106** (2–3), 179–198.
96. Lyashchenko, A.K. and Dunyashev, V.S. (2003) *J. Mol. Liq.*, **106** (2–3), 199–213.
97. Lobyshev, V.I., Solovey, A.B., and Bulienkov, N.A. (2003) *J. Mol. Liq.*, **106** (2–3), 277–297.
98. Botti, A., Bruni, F., Imberti, S., Ricci, M.A., and Soper, A.K. (2005) *J. Mol. Liq.*, **117**, 77–79.
99. Botti, A., Bruni, F., Imberti, S., Ricci, M.A., and Soper, A.K. (2005) *J. Mol. Liq.*, **117**, 81–84.
100. Smith, R.L., Lee, S.B., Homori, H., and Arai, K. (1998) *Fluid Phase Equilib.*, **144**, 315–322.
101. de Maeyer, L. and Kessling, G. (1995) *J. Mol. Liq.*, **67**, 193–210.
102. Ando, K. and Hynes, J.T. (1995) *J. Mol. Liq.*, **64**, 25–37.
103. Guardia, E., Marti, J., Padro, J.A., Saiz, L., and Komolkin, A.V. (2002) *J. Mol. Liq.*, **96–97**, 3–17.
104. Atams, A.A., Atamas, N.A., and Bulavin, L.A. (2005) *J. Mol. Liq.*, **120**, 15–17.
105. Sato, T. and Buchner, R. (2005) *J. Mol. Liq.*, **117**, 23–31.
106. Sciortino, F., Geiger, A., and Stanley, H.E. (1991) *Nature*, **354**, 218–221.
107. Sciortino, F., Geiger, A., and Stanley, H.E. (1992) *J. Chem. Phys.*, **96**, 3857–3866.
108. Kaatzte, U. (2011) *J. Mol. Liq.*, **165**, 105–112.
109. Alder, B.J. and Alley, W.E. (1984) *Phys. Today*, **37**, 56–57.
110. Fuoss, R.M. and Kirwood, J.G. (1941) *J. Am. Chem. Soc.*, **63**, 385.
111. Birshstein, T.M. and Ptitsyn, O.B. (1954) *Zh. Fiz. Khim.*, **24** (1998), 217–222.
112. Marchal, J. and Benoit, H. (1955) *J. Chem. Phys.*, **52**, 818–820.
113. Sebastian, M.T. and Jantunen, H. (2010) *Int. J. Appl. Ceram. Technol.*, **7** (4), 415–434.
114. Gibson, R.F. (2010) *Compos. Struct.*, **92** (12), 2793–2810.
115. Juuti, J., Teirikangas, M., Sonoda, K., and Jantunen, H. (2010) *Int. J. Appl. Ceram. Technol.*, **7**, 452–460.
116. Stuerger, D., and Caillot, T. (2010) Chapter 6 Microwave chemistry and nanomaterials: from laboratory to pilot plant, in *Nanomaterials and Surface Engineering* (ed. J. Takaloum), ISTE-Wiley, London, 163–192.
117. Takadom, J. (2010) *Nanomaterials and Surface Engineering*, ISTE-Wiley, London.
118. Ashjari, M., Mahdavian, A.R., Ebrahimi, N.G., and Mosleh, Y. (2010) *J. Inorg. Organomet. Polym.*, **20**, 213–219.
119. Todd, M.G. and Shi, F.G. (2003) *J. Appl. Phys.*, **94**, 4551–4557.
120. Todd, M.G. and Shi, F.G. (2005) *IEEE Trans. Dielectr. Electr. Insul.*, **12** (3), 601–611.
121. Olmedo, L., Chateau, G., Deleuze, C., and Forville, J.L. (1993) *J. Appl. Phys.*, **73** (10), 6992–6994.
122. Psarras, G.C., Manolakaki, E., and Tsangaris, G.M. (2003) *Compos.: Part A*, **34**, 1187–1198.
123. Wu, L.Z., Ding, J., Jiang, H.B., Chen, L.F., and Ong, C.K. (2005) *J. Magn. Mater.*, **285**, 233–239.
124. Sonoda, K., Juuti, J., Moriya, Y., and Jantunen, H. (2010) *Compos. Struct.*, **92**, 1052–1058.
125. Sonoda, K., Teirikangas, M., Juuti, J., and Jantunen, H. (2011) *J. Magn. Mater.*, **323**, 2281–2286.
126. Alexandre, M. and Dubois, P. (2000) *Mater. Sci. Eng.*, **28**, 1.

127. Ray, S.S. and Okamoto, M. (2003) *Prog. Polym. Sci.*, **28**, 1539–1641.
128. Ray, S.S. and Bousmina, M. (2005) *Prog. Mater. Sci.*, **50**, 962–1079.
129. Fischer, H. (2003) *Mater. Sci. Eng. C*, **23**, 763–772.
130. Burmistr, M.V., Sukhyy, K.M., Shilov, V.V., Pissis, P., Spanoudaki, A., Sukha, I.V., Tomilo, V.I., and Gomza, Y.P. (2005) *Polymer*, **46**, 12226–12232.
131. Fedullo, N., Sorlier, E., Sclavons, M., Bailly, C., Lefebvre, J.M., and Devaux, J. (2007) *Prog. Inorg. Coat.*, **58**, 87–95.
132. Tanaka, T., Montanari, G.C., and Mühlaupt, R. (2004) *IEEE Trans. Dielectr. Electr. Insul.*, **11**, 763–784.
133. Zhang, Y.H., Dang, Z.M., Fu, S.Y., Xin, J.H., Deng, J.G., Wu, J., Yang, S., Li, L.F., and Yan, Q. (2005) *Chem. Phys. Lett.*, **401**, 553–557.
134. Pissis, P. and Kyritsis, A. (1997) *Solid State Ionics*, **97**, 105–113.
135. Pissis, P., Kyritsis, A., Konsta, A.A., and Daoukaki, D. (1999) *Colloids Surf. A*, **149**, 253–262.
136. Shinyashiki, N., Sengwa, R.J., Tsubotani, S., Nakamura, H., Sudo, S., and Yagihara, S. (2006) *J. Phys. Chem. A*, **110**, 4953–4957.
137. Sengwa, R.J. and Sankhla, S. (2007) *Polymer*, **48**, 2737–2744.
138. Sengwa, R.J. and Sankhla, S. (2007) *Colloids Polym. Sci.*, **285**, 1237–1252.
139. Sengwa, R.J. and Sankhla, S. (2007) *J. Macromol. Sci. Part B: Phys.*, **46**, 717–747.
140. Sengwa, R.J. and Sankhla, S. (2007) *J. Mol. Liq.*, **141**, 73–93.
141. Georgousis, G., Kanapitsas, A., Pissis, P., Savelyev, Y.V., Veselov, V.Y., and Privalko, E.G. (2000) *Eur. Polym. J.*, **36**, 1113–1126.
142. Kanapitsas, A., Pissis, P., and Kotsilkova, R. (2002) *J. Non-Cryst. Solids*, **305**, 204–211.
143. Böhning, M., Goering, H., Fritz, A., Brzezinka, K.W., Turkey, G., Schönhals, A., and Scharter, B. (2005) *Macromolecules*, **38**, 2764–2774.
144. Gun'ko, V.M., Pissis, P., Spanoudaki, A., Zarko, V.I., Nychiporuk, Y.M., Andriyko, L.S., Goncharuk, E.V., Leboda, R., SkubiszewskaZieba, J., Osovskii, V.D., and Ptushinskii, Y.G. (2007) *J. Colloid Interface Sci.*, **312**, 201–213.
145. Mijović, J., Lee, H., Kenny, J., and Mays, J. (2006) *Macromolecules*, **39**, 2172–2175.
146. Bur, A.J., Lee, Y.H., Roth, S.C., and Start, P.R. (2005) *Polymer*, **46**, 10908–10920.
147. Noda, N., Lee, Y.H., Bur, A.J., Prabhu, V.M., Snyder, C.R., Roth, S.C., and McBrearty, M. (2005) *Polymer*, **46**, 7201–7212.
148. Davidson, D.W. (1966) *Molecular Relaxation Processes*, Special Publication No. **20**, Chemical Society, London.
149. Asami, K. (2002) *Prog. Polym. Sci.*, **27**, 1617–1659.
150. Feldman, Y., Ermolina, I., and Hayashi, Y. (2003) *IEEE Trans. Dielectr. Electr. Insul.*, **10**, 728–753.
151. Cametti, C. (2009) *Riv. Nuovo Cimento*, **32**, 185–260.
152. Errera, J. (1926) *Colloid Science*, Vol. **2**, Chemical Catalog Co., New York.
153. Schwan, H.P. (1957) *Adv. Biol. Med. Phys.*, **5**, 147–149.
154. Lyklema, J. and Van Leeuwen, H.P. (1999) *Adv. Colloid Interface Sci.*, **83**, 33–46.
155. O'Brien, R.W. (1986) *J. Colloid Interface Sci.*, **113**, 81–88.
156. Hussain, S., Youngs, I.J., and Ford, I.J. (2004) *J. Phys. D: Appl. Phys.*, **37**, 318–325.
157. Bonincontro, A. and Cametti, C. (2004) *Colloids Surf. A*, **246**, 115–120.
158. Buchner, R., Baar, C., Fernandez, P., Schrödl, S., and Kunz, W. (2005) *J. Mol. Liq.*, **118**, 179–187.
159. Jönsson, P.E., Garcia-Palacios, J.L., Hansen, M.F., and Nordblad, P. (2004) *J. Mol. Liq.*, **114**, 131–135.
160. Yu, X. and Somasundaran, P. (1996) *J. Colloid Interface Sci.*, **177**, 283–287.
161. Saveyn, H., Meersseman, S., Thas, O., and Van der Meeren, P. (2005) *Colloids Surf. A*, **262**, 40–46.
162. Ayol, A., Dentel, S.K., and Filibeli, A. (2004) *Water Sci. Technol.*, **50**, 9.
163. Eriksson, L., Alm, B., and Stenius, P. (1993) *Colloids Surf. A*, **70**, 47–60.
164. Gregory, J. (1973) *J. Colloid Interface Sci.*, **42**, 448–456.

165. Dickinson, E. and Eriksson, L. (1991) *Adv. Colloid Interface Sci.*, **34**, 1–34.
166. Borget, P., Lafuma, F., and Bonnet-Gonnet, U. (2005) *J. Colloid Interface Sci.*, **284**, 560–570.
167. Oulanti, O., Widmaier, J., Pefferkorn, E., Champ, S., and Auweter, H. (2006) *J. Colloid Interface Sci.*, **294**, 95–103.
168. Neyret, S., Ouali, L., Candau, F., and Pefferkorn, E. (1995) *J. Colloid Interface Sci.*, **176**, 86–94.
169. Aoki, K. and Adachi, Y. (2006) *J. Colloid Interface Sci.*, **300**, 69–77.
170. Runkana, V., Somasundaran, P., and Kapur, P.C. (2006) *Chem. Eng. Sci.*, **61**, 182–193.
171. Stoll, S. and Buffle, J. (1996) *J. Colloid Interface Sci.*, **180**, 548–563.
172. Stoll, S. and Buffle, J. (1998) *J. Colloid Interface Sci.*, **205**, 290–304.
173. Runkana, V., Somasundaran, P., and Kapur, P.C. (2004) *J. Colloid Interface Sci.*, **270**, 347–358.
174. Gregory, J. (1988) *Colloids Surf.*, **31**, 231–253.
175. Abu-Orf, M.M. and Dentel, S.K. (1999) *J. Environ. Eng. ASCE*, **125**, 1133–1147.
176. Hollingsworth, A.D. and Saville, D.A. (2004) *J. Colloid Interface Sci.*, **272**, 235–245.
177. Tirado, M.C., Arroyo, F.J., Delgado, A.V., and Grosse, C. (2000) *J. Colloid Interface Sci.*, **227**, 141–146.
178. Myers, D.F. and Saville, D.A. (1989) *J. Colloid Interface Sci.*, **131**, 461–470.
179. Schwan, H.P., Schwarz, G., Maczuz, J., and Pauly, H. (1962) *J. Phys. Chem.*, **166**, 2626–2632.
180. Carrique, F., Zurita, L., and Delgado, A.V. (1994) *Colloids Surf. A*, **92**, 9–21.
181. Barchini, R. and Saville, D.A. (1995) *J. Colloid Interface Sci.*, **173**, 86–91.
182. Dukhin, S.S. and Shilov, V.N. (1974) *Dielectric Phenomena and the Double Layer in Disperse Systems and Polyelectrolytes*, John Wiley & Sons, Inc., New York.
183. DeLacey, E.H.B. and White, L.R. (1981) *J. Chem. Soc., Faraday Trans.*, **77**, 2007.
184. Genz, U., Helsen, J.A., and Mewis, J. (1994) *J. Colloid Interface Sci.*, **165**, 212–220.
185. Pribush, A., Meiselman, H.J., Meyerstein, D., and Meyerstein, N. (1999) *Biorheology*, **36**, 411–415.
186. Pribush, A., Meiselman, H.J., Meyerstein, D., and Meyerstein, N. (2000) *Biorheology*, **37**, 429–435.
187. Christensen, P.V. and Keiding, K. (2008) *J. Colloid Interface Sci.*, **327**, 362–369.
188. Christensen, P.V., Christensen, M.H., and Keiding, K. (2009) *J. Colloid Interface Sci.*, **340**, 46–52.
189. Christensen, P.V., Hinge, M., and Keiding, K. (2011) *J. Colloid Interface Sci.*, **356**, 681–689.
190. Christensen, P.V. and Keiding, K. (2009) *J. Colloid Interface Sci.*, **340**, 46–52.
191. Jiménez, M.J. and Bellini, T. (2010) *Curr. Opin. Colloid Interface Sci.*, **15**, 131–144.